Multistep Reversible Redox Systems, LXVII[∓]

2,5-Disubstituted *N,N'*-Dicyanobenzoquinonediimines (DCNQIs): Charge-Transfer Complexes and Radical-Anion Salts and Copper Salts with Ligand Alloys: Syntheses, Structures and Conductivities

Siegfried Hünig,*[a] Martina Kemmer,[a] Hubert Meixner,[a][2] Klaus Sinzger,[a][2] Hermann Wenner,[a] Thomas Bauer,[b][∓∓] Ekkehart Tillmanns,[b][∓∓] Franz Rudolf Lux,[c] Michael Hollstein,[c] Hans-Georg Groß,[d] Uwe Langohr,[d] Hans-Peter Werner,[d] Jost Ulrich von Schütz,[d] and Hans-Christoph Wolf[d]

The new members of the series of 2,5-disubstituted DCNQIs, **1d** (Cl/OMe), **1e** (Br/OMe), **1j** (Cl/I), **1k** (Br/I), **1l** (I/I), form conducting charge-transfer complexes with TTF (tetrathiofulvalene) which are comparable to known DCNQI/TTFs. From these DCNQIs highly conducting radical-anion salts [2-X, 5-Y-DCNQI]$_2$M (M = Li, Na, K, NH$_4$, Tl, Rb, Ag, Cu) can also be prepared either from the DCNQIs and MI (not AgI), on a metal wire (Ag, Cu), or by electro-crystallization (M = Tl, Ag, Cu). For better crystals a method using periodical switching between reduction and partial oxidation has been developed. With CF$_3$ (large, strongly electron-attracting) as the substituent in DCNQIs **1m** (OMe/CF$_3$) and **1n** (Me/CF$_3$), conducting TTF complexes remain whereas only **1n** yields an insulating copper salt. DCNQI–Cu salts with high conductivities are obtained with alloys containing two or three different DCNQIs. The temperature-dependent conductivities of DCNQI–M salts (other than copper) are similar to those of metal-like semiconductors. All new DCNQI–Cu salts are metallic [M] down to low temperatures, except [**1d** (Cl/OMe)]$_2$Cu which undergoes a sharp phase transition to an insulating state[M → I]. By variation of the ligands or their ratios in conducting alloys of DCNQI–Cu salts temperature-dependent conductivities can be tuned from M → I to M. In addition, alloying three ligands produced for the first time a radical salt with temperature-independent conductivity from 5 to 300 K. Most remarkably, alloys of the type [(2,5-Me$_2$DCNQI)$_m$] Cu/[{2,5-(CD$_3$)$_2$-DCNQI}$_n$]$_2$Cu which exhibit a sharp M → I phase transition on further cooling reenter the conducting state by an I → M transition, with changes of ca. 10^8 Scm^{-1} both ways. For the first time in the field of organic metals crystal structures of DCNQI–copper salts have been determined by X-ray powder diffraction methods and refined by Rietveld analysis. Unit cell data, coordination angles and distances of the π planes are in excellent agreement with the single-crystal X-ray data. However, bond lengths and angles of the ligands are to be less accurate. This powder method proves to be most valuable if only microcrystalline material is available.

The discovery of electrical conducting solids based on tetrathiofulvalene[1−3] has triggered an avalanche of research for new suitable materials up to the present. The interest has been focussed both on the understanding of this unusual phenomenon and on tailoring compounds for practical applications.[4]

Although the basic requirements for conductivity of low molecular organic solids are now clear a more detailed understanding of the interplay of molecular geometry, crystal structure and conductivity (together with its temperature dependence) was hampered by the differing crystal lattices of the various materials. This situation changed with the discovery of (substituted) *N,N*-dicyanoquinoneimines (DCNQIs).[5] Especially radical-anion salts of 2,5-disubstitued DCNQIs prefer all the same space group *I*4$_1$/*a* (or a closely related one) and therefore allow a comparison of their properties.

Thus very subtle substituent effects are translated in minor variations of the basic crystal lattice with definite changes in temperature-dependent conductivities, allowing a much more detailed understanding of this interplay.[6]

We therefore set out to explore the limit of this generalization in the papers of this series.

In a preceding paper we described a variety of new 2,5-disubstituted DCNQIs, together with their redox properties.[8] We now conclude our research activities in this field by posing the following questions arising from the already accumulated experience:

(1) Will the additional examples of 2,5-disubstituted DCNQIs presented here produce charge-transfer complexes

and radical-anion salts with properties similar to those already described, especially in the presence of the large and strongly electron-attracting CF_3 substituent?

(2) Can the growth of single crystals by electrocrystallization be improved by rhythmic reversal of the current flow?

(3) Which variations are tolerated for ligand alloying in DCNQI−Cu salts with two different 2,5-disubstituted DCNQIs (ratio and pattern)?

(4) Will the temperature-dependent conductivities of those alloyed copper salts mimic those of the two single copper salts or will new properties arise, especially with respect to phase transitions?
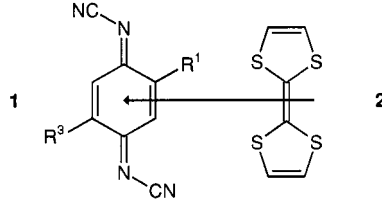
(5) Which structural data for DCNQI−Cu salts can safely be derived from powder-diffraction data refined by Rietveld analysis (so far rarely applied to organic solids) compared to single-crystal X-ray data?

The following sections concentrate mainly on answering these questions.

Charge-Transfer Complexes of DCNQIs 1a−n with TTF

As with other 2,5-disubstituted DCNQI[9] derivatives, 1a−n immediately form black microcrystalline charge-transfer complexes on mixing their solutions in acetonitrile or dichloromethane with those of TTF (2). The stoichiometry in all the examples listed in Table 1 was found to be 1:1.

Table 1. Charge-transfer complexes 1:1 from DCNQIs (1) and TTF (2) together with their powder conductivities σ [Scm^{-1}]

1	R^1	R^3	Yield	m.p.	σ	Ref.
			(%)	[°C][b]	[S cm^{-1}]	
a	OMe	OMe	60	199	5×10^{-2}	[c]
b	Me	OMe	54	118	2×10^{-2}	[c]
c	Me	Me	52	114	$< 10^{-7}$	[c]
d	Cl	OMe	93	155	3×10^{-2}	[d]
e	Br	OMe	75	160	3×10^{-2}	[d]
f	I	OMe	74	122	2×10^{-2}	[d]
g	Cl	Me	98	144	2×10^{-1}	[c]
h	Br	Me	87	129	6×10^{-1}	[c]
i	I	Me	75	144	3×10^{-2}	[c]
j[a]	Cl	I	77	125	1×10^{-3}	[d]
k[a]	Br	I	78	127	2×10^{-2}	[d]
l[a]	I	I	83	152	2×10^{-3}	[d]
m	OMe	CF$_3$	95	212	1×10^{-3}	[d]
n	Me	CF$_3$	90	198	1×10^{-2}	[d]

[a] Physical data of the DCNQIs, see ref.[9] − [b] Determined by DTA. − [c] Ref.[10] − [d] This paper.

The rather high powder conductivities $(10^{-1}-10^{-3}$ Scm^{-1}) of the new complexes correlate well with those of

the complexes already reported.[9] Together with their total absorption in the infrared these data point to segregated stacks of two components. However, this arrangement is kinetically controlled since, e.g. growing single crystals of 1a·2, 1h·2, and 1i·2 affords insulating charge-transfer complexes with mixed stacks.[10] It is remarkable that despite the wide range of redox potentials of the DCNQIs from $E_2 = 0.15$ V of 1a (OMe/OMe) to $E_2 = 0.63$ V of 1l (I/I) charge-transfer complexes with TTF can be obtained, even with the same stoichiometry. However, for $E_2 = 0.83$ V, the potential of the DCNQI with R^3, R^5 = CF$_3$,[8] no charge-transfer complex with TTF could be isolated, probably due to total electron transfer to the acceptor (see ref.[11][13]). If solubilities allow, hot acetonitrile is to be preferred to dichloromethane for high-potential DCNQIs.[11−13]

In accord with $E_2 = +0.53$ V for 1m (R^1 = OMe, R^3 = CF$_3$) and $E_2 = +0.55$ V for 1n (R^1 = Me, R^3 = CF$_3$) both donors yield 1:1 complexes with TTF of normal conductivities. Slight deviations from the ideal 1:1 stoichiometry may either be interpreted as due to experimental errors in the combustion analysis or defective crystal growth.[13] Obviously, the rather large diameter of the CF$_3$ group (5.2 to 5.6 Å) does not interfere with the close packing of the π planes in the acceptor stacks, a prerequisite for conductivity. The CF$_3$ groups of neighbouring molecules are probably interlocked like cog wheels, similar to the acceptor itself,[8] thereby diminishing their actual size.

Radical-Anion Salts [DCNQI]$_2$M with Monovalent Cations

Quionoid acceptors such as DCNQIs can generally be transformed into their radical-anion salts by three methods.
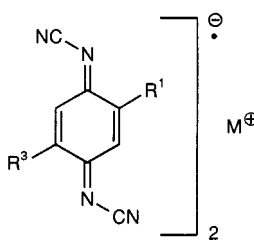
Preparation from Metal Iodides

The use of metal iodides as electron donors and their subsequent successful application to TCNQs has already been described by Melby.[17] Consequently, iodides have also been employed for various DNCQIs.[18] We now describe further radical-anion salts of the stoichiometry [2-X,5-Y-DCNQI]$_2$M with M = Li, Na, K, NH$_4$, Rb and Cu produced by this method. Without special precautions the black salts are formed as microcrystalline powders (Table 2).

This simple and quick method is applicable to a remarkably broad variety of 2,5-substituted DCNQIs as well as to different metal ions. With one exception (1n·Rb) all salts display powder conductivities up to 1 to 10^{-3} Scm^{-3} from which single-crystal conductivities up to 1000^{-1} Scm^{-1} can be expected (vide infra).

Preparation from Metal Wire

DCNQI radical-anion salts of copper and silver can be most easily prepared from DCNQIs and the corresponding

Table 2. Microcrystalline radical-anion salts 1_2M from DCNQIs **1** and metal or ammonium iodides; yields (%), melting points (m.p. [°C]) by DTA and powder conductivities σ [S cm^{-1}]

	R^1	R^3	M	Yield (%)	m.p. [°C]	σ [S cm^{-1}]
a	OMe	OMe	Li[a]	88	211	7×10^{-2}
			Na[b]	35	198	2×10^{-3}
			K	94	170	2×10^{-2}
			NH$_4$	dec.	—	—
			Rb	58	170	1×10^{-4}
			Cs	[c]	—	—
			Cu	67	243	2×10^{-2}
b	Me	OMe	Li[d]	73	64[e]	[f]
			Na	100	140	3×10^{-3}
			K	[g]	—	—
			NH$_4$	dec.	—	—
			Rb	70	90	3×10^{-3}
			Cu[h]	82	166	4×10^{-2}
c	Me	Me	Li[b]	100	192	—
			Na[b]	88	176	—
			K[b]	96	176	—
			NH$_4$	44	129	1×10^{-1}
			Rb[b]	69	160	—
			Cs	[i]	—	—
			Cu[j]	100	201	0.4
d	Cl	Me	Li[a]	56	76[d]	1.0
			Cu	96	180	2×10^{-2}
e	Br	OMe	Li[f]	—	—	—
			Cu	98	176	2×10^{-2}
f	I	OMe	Cu	47	n.d.	4×10^{-2}
h	Br	Me	NH$_4$	85	134	2×10^{-2}
i	I	Me	NH$_4$	77	134	4×10^{-2}
j	Cl	I	Cu	72	150	3×10^{-2}
k	Br	I	Cu	74	164	2×10^{-2}
l	I	I	Cu	91	164	2×10^{-2}
m	OMe	CF$_3$	Cu	[f]	—	—
n	Me	CF$_3$	Cu	62	n.d.	1×10^{-3}

[a] Contains 1 H$_2$O. − [b] Ref.[14−16,18] − [c] **1a** reisolated. − [d] Contains 1.8 H$_2$O. − [e] Decomposition. − [f] Varying data. − [g] Green solution. − [h] Ref.[18] − [i] Blue solution. − [j] Ref.[6]

metal wire in acetonitrile yielding very often single crystals of good quality.[12]

For the variety of DCNQIs described in the previous paper[8] this method has already been discussed.[14] For comparison of their conductivities with radical salts obtained by the other methods, some earlier results are also included here (Table 3).

Conductivities of these salts agree completely with those of samples prepared from metal wire and by electrocrystallization, as is to be expected from earlier results, thereby confirming the same structural features.[12]

Preparation by Electrocrystallization

The most widely used technique of electrocrystallization was also applied to a variety of DCNQIs listed in Table 4.

Table 3. Radical-anion salts (DCNQI)$_2$M(Cu, Ag) grown in acetonitrile on a metal wire in solutions of the DCNQIs **1** and CuBr$_2$ or AgNO$_3$, respectively, and their single-crystal (s) or powder (p) conductivities [S cm^{-1}]

DCNQI **1** R^1/R^3	M	Yield (%)	Needles [mm]	σ [S cm^{-1}]
1a OMe/OMe	Cu[a]	48	1	(p) 0.1
1b Me/OMe	Cu[a]	70	10	(p) 0.1
1c Me/Me	Ag	98	8	(p) 6×10^{-2}
1d Cl/OMe	Cu	68	5	(s) 500
1e Br/OMe	Cu	87	25	(s) 500
1h Br/Me	Ag	98	15	(s) 22
1i I/Me	Ag	85	10	(p) 2×10^{-2}
1j Cl/I	Cu	—	fur	—
	Ag	60	3	(p) 3×10^{-3}
1k Br/I	Cu	87	4	(p) 1×10^{-2}
	Ag	51	3	(p) 6×10^{-3}
1l I/I	Cu	—	fur	(p) 2×10^{-2}

[a] Ref.[19]

Besides some new, highly conducting DCNQI copper salts (**1b**, **1d**, **1e**, **1f**), radical-anion salts with cations rubidium (**1a**), thallium (**1c**[20], **1h**, **1i**), and silver (**1k**) could also be prepared.

Table 4. Radical-anion salts (DCNQI)$_2$M by electrolysis of DCNQIs **1** in acetonitrile in the presence of A = (RbClO$_4$), B = (CF$_3$CO$_2$Tl), C = [Cu(CH$_3$CN)$_4$ClO$_4$], D = (AgNO$_3$). Current I = 9−10 µA (A, C, D), 20−30 µA (B): Yields, lengths of the crystal needles and single-crystal (s) and powder (p) conductivities [S cm^{-1}]

DCNQI **1** R^1/R^3	M	A, B C, D	Yield (%)	Needles [mm]	σ [S cm^{-1}]
1a OMe/OMe	Rb	A	29	3[a][f]	(p) 1×10^{-4}
	Cu	C	20	15	(s) 700[c]
1b Me/OMe	Cu	C	23	15[b]	(s) 80
1c Me/Me	Tl	B	48	6	(s) 50[d]
1d Cl/OMe	Cu	C	34	5	(s) 500
1e Br/OMe	Cu	C	39	7	(s) 500
1f I/OMe	Cu	C	8	3[b][f]	(p) 4×10^{-2}
1h Br/Me	Tl	B	22	3	—
1i I/Me	Tl	B	28	3[b]	—
1j Cl/I	Cu	C	29	10[b]	(s) 70[e]
1k Br/I	Cu	C	50	8	(s) 500
	Ag	D	21	2	—
1l I/I	Cu	C	45	15[b]	(s) 70[e]

[a] Cubes. − [b] Bushels of very thin needles. − [c] Ref.[19] − [d] Ref.[20] − [e] Microwave measurements. − [f] Current switching 70:30 s^{-1}, see this paper.

The rather low conductivities of 70 Scm^{-1} measured for (**1f**)$_2$Cu and (**1l**)$_2$Cu compared to 500 Scm^{-1} for (**1k**)$_2$Cu are probably due to the microwave techniques which had to be used for these very thin needles. Evaluations by this method are based on the exact dimensions of the sample which could not be determined in our material with sufficient accuracy.[21]

Sometimes, even electrocrystallization yields only microcrystalline material, in spite of the systematic variation of solvent, supporting electrolyte, concentration, temperature, and density of the current. In this situation, rhythmic reversal of the current flow in the electrochemical cell (see circuit diagram, Figure 13) may be helpful. This procedure is based

on the common fact that small crystals dissolve faster than large ones due to their more extended surface. From a microcrystalline material at the electrode, the smallest particles should therefore dissolve faster on reversing the current flow for a certain time. In this way, on normal current flow, new material should be deposited on the larger crystals which finally grow at the cost of the smaller ones. Indeed,

single crystals of good quality were easily obtained for [2,5-(MeO)$_2$DCNQI]$_2$Cu, (**1b**)$_2$Cu and [2-I,5-(MeO)DCNQI]$_2$-Cu, (**1f**)$_2$Cu by current switching 70:30/s.

This method, disclosed here for the first time, may be advisable also for other types of electrocrystallizations.

Tables 2−4 clearly demonstrate that whenever solid DCNQI radical salts are obtained electric conductivity is

Table 5. Copper salts from two different 2,5-disubstituted DCNQIs (**1**) (1:1); single crystals grown on a copper wire in acetonitrile containing CuBr$_2$ during 2−4 d

No.	1	DCNQIs R^1/R^3 (m)	Yield Cu salt (%)	m/n[a]	m.p.[b] [C°]	σ[c] [S cm^{-1}]	C calcd. found	H	N	Cu
1	a	OMe/OMe	99	1.0:1.0	185	(s) 220	51.77	3.43	24.16	13.70
	c	Me/Me					51.84	3.51	23.91	14.10
2	a	OMe/OMe	86	0.6:1.4	183	(s) 220	41.21	2.20	20.68	
	c	Br/Me					41.55	2.08	20.44	
3	a	OMe/OMe	76	0.7:1.3	185	(s) 180	37.79	2.07	18.81	
	c	I/Me					38.04	1.99	18.81	
4	b	Me/OMe	48	0.8:1.2	173	(s) 40	54.01	3.63	25.20	14.29
	c	Me/Me					53.72	3.60	25.41	13.66
5	b	Me/OMe	41	1.0:1.0	170	2 × 10^{-1}	44.29	2.56	21.85	
	h	Br/Me					44.29	2.44	21.89	
6	b	Me/OMe	98	1.2:0.8	195	(s) 260	42.65	2.54	20.73	11.75
	i	I/Me					42.50	2.41	20.89	11.30
7	b	Me/OMe	50	1.4:0.6	175	4 × 10^{-1}	33.15	1.23	17.99	
	p	Br/Br					33.30	1.36	17.53	
8	c	Me/Me	96	1.2:0.8	173	(s) 180	45.93	2.71	22.38	
	e	Br/OMe					45.79	2.50	22.41	
9	c	Me/Me	93	0.9:1.1	191	3 × 10^{-1}	49.95	2.82	24.66	13.99
	g	Cl/Me					50.14	2.95	24.14	14.23
10	c	Me/Me	92	1.1:0.9[d]	197	2 × 10^{-1}	46.78	2.79	22.86	11.74
	h	Br/Me					46.82	2.58	22.76	12.96
11	c	Me/Me	90	1.0:1.0	192	2 × 10^{-1}	41.96	2.42	20.61	11.68
	i	I/Me					42.48	2.52	20.76	11.89
12	c	Me/Me	94	1.0:1.0	191	(s) 130	45.73	2.14	23.71	13.44
	o	Cl/Cl					45.48	2.05	23.11	13.57
13	c	Me/Me	85	1.1:0.9	180	3 × 10^{-1}	42.97	2.10	22.03	
	q	Cl/Br					42.97	1.93	22.29	
14	c	Me/Me	82	1.0:1.0	187	−	38.49	1.80	19.96	
	p	Br/Br					38.06	1.60	19.86	
15	e	Br/OMe	61	0.2:1.8	192	2 × 10^{-1}	38.27	1.79	19.84	
	h	Br/Me					38.33	1.71	19.97	
16	g	Cl/Me	99	1.0:1.0	187	2 × 10^{-1}	41.79	1.95	21.66	
	h	Br/Me					41.76	1.90	21.90	
17	g	Cl/Me	95	0.5:1.5	191	(s) 340	41.69	1.95	21.62	
	i	I/Me					42.05	1.89	21.62	
18	g	Cl/Me	75	0.8:1.2	183	(s) 230	40.58	1.30	22.54	
	o	Cl/Cl					40.43	1.39	21.80	
19	g	Cl/Me	97	1.0:1.0	172	−	37.97	1.31	20.85	
	q	Cl/Br					38.04	1.41	20.40	
20	g	Cl/Me	41	1.1:0.9	188	2 × 10^{-1}	35.96	1.29	19.62	
	p	Br/Br					35.96	1.28	19.02	
21	h	Br/Me	85	1.0:1.0[e]	185	1 × 10^{-1}	35.51	1.66	18.41	
	i	I/Me					35.41	1.81	18.28	
22	h	Br/Me	84	1.0:1.0	174	1 × 10^{-1}	37.97	1.31	20.84	
	o	Cl/Cl					38.13	1.32	20.56	
23	h	Br/Me	88	1.0:1.0	175	2 × 10^{-1}	35.07	1.21	19.25	
	q	Cl/Br					35.48	1.34	18.99	
24	h	Br/Me	83	1.0:1.0	180	2 × 10^{-1}	32.58	1.13	17.89	
	p	Br/Br					32.55	1.19	17.39	
25	i	I/Me	89	1.0:1.0	176	(s) 280	34.92	1.21	19.17	
	o	Cl/Cl					36.28	1.26	19.29	
26	i	I/Me	80	1.3:1.7	175	(s) 110	31.17	1.21	16.79	
	p	Br/Br					30.92	0.98	17.07	
27	a	OMe/OMe	81	0.6	186	(s) 70	44.26	2.93	20.89	
	c	Me/Me		0.8			43.95	2.61	21.36	
	i	I/Me		0.6						

[a] Calculated from elemental analysis. − [b] By DTA. − [c] (s) single crystal, otherwise powder. − [d] 7 d; neutron activation: A/B = 0.90:1.10, calcd. Br = 17.46, Cu = 12.62; found Br = 17.75, Cu = 12.32. − [e] Neutron activation A/B = 1.15:0.85, calcd. Br = 15.27, Cu = 10.56; found Br = 15.15, Cu = 10.61.

observed also. As well two large substituents of opposite electronic properties (OMe/OMe or I/I) are tolerated as two substituents strongly differing in size with equal (e.g. MeO/Me or Cl/I) or opposite electronic effects (Cl/OMe or I/Me). This great variability fortunately is connected especially with copper as gegenion (metallic conductivity[6][7]). By contrast, thallium[20] yielded a solid radical salt with **1c** (Me/Me) only. Conductivity data from crystal powder (p) are much less reliable than those obtained from single crystals (s) [cf. **1a**Cu: 0.1 Scm^{-1} (p), 700 Scm^{-1} (s)[19] vs. **1b**Cu: 0.1 Scm^{-1} (p), 80 Scm^{-1} (s)]. The accuracy of powder data suffer both from the method of measurement (compression between two electrodes) and the variable surface properties of the microcrystals.

Ligand Alloys in Copper Salts of 2,5-Disubstituted DCNQIs

As demonstrated earlier[15,16,22−27] and in this paper (vide infra), radical-anion salts of the general type [2-X,5-Y-DCNQI]$_2$Cu all crystallize in the highly symmetrical space group $I4_1/a$ in spite of the strong variation of the substituents and redox potentials of the DCNQI ligands. One group of these salts shows metallic conductivity down to low temperatures (M), whilst others possess a phase transition to an insulating state at various temperatures (M → I).

Because of the great variability in the 2,5-substituent pattern, two or even three different 2,5-disubstituted DCNQIs may form an alloy of ligands in the stacks of DCNQI−Cu salts. A study of the properties of these alloys could lead to a better understanding of the substituent dependence of electric conductivity and the temperature of phase transitions.[28]

For the preparation of the mixed DCNQI−Cu salts, a copper wire was immersed into a solution of different DCNQIs (1:1 and 10:1:1) in acetonitrile in the presence of copper(II) bromide. In this way, 26 binary and one ternary salt were isolated (Table 5).

In most cases the ratios of the components in the mixed DCNQI−Cu salts are close to those in the starting solution, namely 1:1. These ratios are calculated from the elemental analyses which are also given in Table 5. Their accuracy should not be overestimated, as can be judged from two examples where comparison with probably more precise results from neutron activation analysis (NAA) (Br, Cu, vide infra) was possible. In entry 10 the ratio 1.1:0.9 is reversed to 0.9:1.1 by NAA. Similarly in entry 21 the ratio 1.0:1.0 changes to 1.15:0.85 by NAA.

The 1:1 ratio of the two different DCNQI ligands was only expected for combinations with similar redox potentials. However, they are obviously not important for the composition of the alloys, as can be exemplified by entry 14. Although $E_2 = +0.21$ V of 2,5-Me$_2$DCNQI[30] and $E_2 = +0.62$ V of 2,5-Br$_2$DCNQI[29] differ by as much as 400 mV the copper salt contains the ligands in a ratio of 1:1, whereas a large excess of 2,5-Br$_2$DCNQI is to be expected. The different rates of crystal growth and solubility,

which are well known from the single component salts (see Tables 3 and 4), probably outweigh the differences in reducibility. This rationalization is in line with the exceptional ratios 1.4:0.6 (entry 2), 1.8:0.2 (entry 15), and 0.5:1.5 (entry 17) where the faster growing component is the preferred one. On this basis, however, the ratio 0.6:1.4 (entry 7) should be reversed.

Electrochemical generation of DCNQI−Cu alloys was used for three different pairs of DCNQIs with varying ratios of the two acceptors. The intention was to create a series of different alloys from the same pair of DCNQIs. This was indeed possible, as can be judged from Table 6, e.g. from 2,5-Me$_2$DCNQI (**1c**) and 2-Br,5-MeDCNQI (**1h**) ten different mixed copper salts were obtained with ligand ratios from 1.95:0.5 to 0.10:1.9 (Table 1 of the supporting information comprises 22 entries). The ratios were again calculated from the elemental analyses. In samples which contained a bromine substituent, however, the crystals were irradiated with a neutron source and the amount of bromine and copper determined from the half life of their radioactive isotopes (NAA). The percentage of the bromine-substituted ligand can be calculated from the constant stoichiometry [DCNQI]$_2$Cu. In eleven alloys the ratio of the two ligands could be calculated in both ways. These ratios agree reasonably well, the NAA data (± 0.2%) being more reliable. The ratio of the ligands in different alloys reflects the ratio of the corresponding DCNQIs in solution but not in a linear way, as demonstrated in Figure 1.
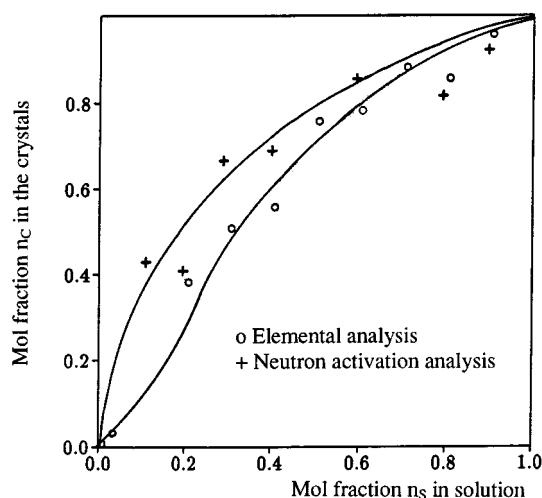

Figure 1. Correlation of the mol fractions of the products [(2,5-Me$_2$DCNQI)$_m$(2-Br,5-MeDCNQI)$_n$]Cu (n_C) with those of the corresponding DCNQIs in the solution for electrocrystallization (n_S)

This correlation agrees well with that of a similar investigation on the same system.[31]

The DCNQI−Cu salts generated both electrochemically and at a copper wire represent alloys with statistically distributed ligands and not crystals with domains of the two DCNQIs or even crystal mixtures of the individual salts. This conclusion can be drawn from the following results:[32] (a) Different crystals of the same mixed salt produce identical mass spectra with the same pattern; (b) in X-ray powder diagrams (vide infra) of the system [[2-Cl,5-

MeDCNQI)$_m$(2-I,-5-MeDCNQI)$_n$]$_2$Cu reflections appear which do not occur in the copper salts of the two components; the rather broad reflections, however, point to strong disorder in the crystal structure; (c) temperature-dependent single-crystal conductivities of two halves of a needle from [(2,5-Me$_2$DCNQI)$_{1.57}$(2-I,5-MeDCNQI)$_{0.43}$]Cu are identical. The existence of large domains of the two ligands is therefore improbable.

All isolated alloys have in common a total absorption between 4000 and 600 cm^{-1} indicating a high powder conductivity of > 0.2 Scm^{-1}.

Deuterated DCNQIs in Alloys of Copper Salts

In 2,5-Me$_2$DCNQI (**1c** ≡ **1c·H$_8$**) the two methyl groups can be replaced by trideuteriomethyl groups, yielding 2,5-(CD$_3$)$_2$DCNQI (**1c·D$_6$**).[3] Since (**1c·D$_6$**)$_c$Cu displays an unprecedented giant secondary isotope effect in its temperature-dependent conductivity (Δσ = 10^8 Scm^{-1})[29][32] the behaviour of alloys of [**1c·H$_8$**]$_2$Cu and [**1c·D$_6$**]$_2$Cu was of special interest. Mixtures of **1c·H$_8$** and **1c·D$_6$** in ratios from 90:10 to 10:90 (10% intervals) were therefore employed in order to grow the corresponding copper salts by electrocrystallization. Because of the extremely small differences between the two ligands the composition of the alloys {(2,5-Me$_2$DCNQI)$_m$[2,5-(CD$_3$)$_2$DCNQI]$_n$}$_2$Cu are assumed to represent the ratio of the two acceptors in solution. These alloys of DCNQI copper salts very often display a pattern of temperature-dependent conductivity which cannot be achieved by employing the corresponding salts containing only one of DCNQI ligands of the alloy (vide infra).

Temperature-Dependent Conductivity of DCNQI Radical-Anion Salts

Most valuable information can be drawn from the temperature dependence of conductivity, especially concerning semi- or metallic conduction and phase transitions. The following background has to be presented here because otherwise the very special effects observed with alloyed DCNQI copper salts could not be appreciated.

Non-Copper Salts

Silver and alkali salts of 2,5-disubstituted DCNQIs so far known have already been demonstrated to behave as "metal-like semiconductors"[35] of low dimensionality.[12,25,27,36] On cooling, the conductivity of solids of this type remains nearly constant, but finally they become insulators at very low temperatures (4-K$_f$ transition,[37] Peierls distortion[38]). The existence of an additional 2-K$_f$ transition (spin-Peierls transformation[39]) between ca. 80 and 100 K can be deduced from their high-resolution IR spectra
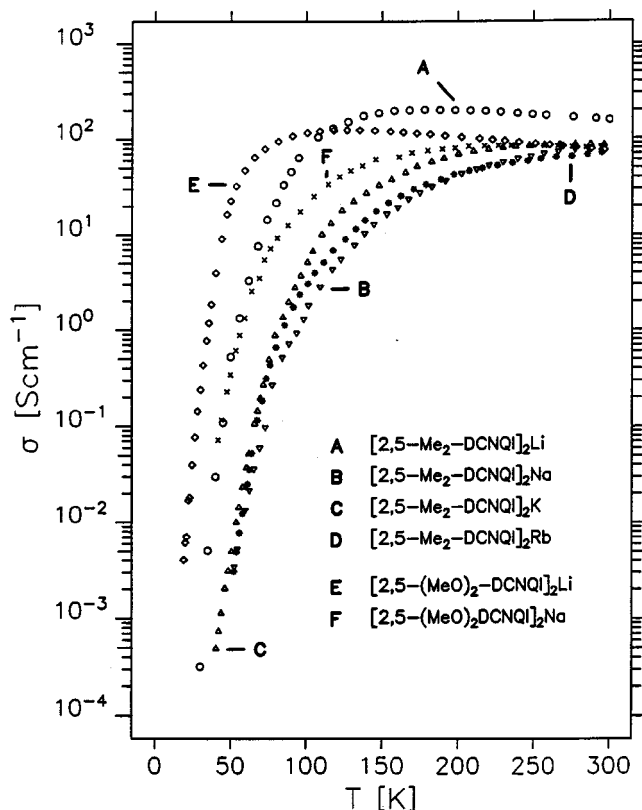

Figure 2. Temperature-dependent single-crystal conductivities of [2,5-Me$_2$DCNQI]$_2$M (M = Li, Na, K, Rb) and [2,5-(MeO)$_2$DCNQI]$_2$M (M = Li, Na)

but is not observed as a change in conductivity.[40] Figure 2 shows the temperature-dependent conductivity of various alkali metals with two sets of DCNQI ligands under identical conditions.[41]

Starting from similar conductivities (ca. 80−180 Scm^{-1}) at ambient temperature their turn to lower conductivity strongly depends on the size of the alkali ion: Rb > K > Na >> Li. In the case of [2,5-Me$_2$DCNQI]$_2$Li a slight increase in conductivity is even observed down to ca. 150 K. However, the larger and more strongly donating methoxy groups extend the range of high conductivity down to even lower temperatures. The lowest temperature for high conductivity so far observed for a non-copper DCNQI salt has been determined to be ca. 70 K for [2,5-(MeO)$_2$-DCNQI]$_2$Li.[41]

The temperature-dependent conductivity of the thallium salt [2,5-Me$_2$DCNQI]$_2$Tl has already been extensively discussed.[20] The temperature/conductivity pattern resembles that of the potassium salt in Figure 2 and that of the corresponding silver salt.[42] Although in the thallium salt the Tl−N≡C− distances are normal (sum of the van der Waals radii 309 pm) this compound is the only one (apart from the DCNQI−Cu salts) which displays a definite knight shift[43] of the ^{205}Tl$^+$ ion. Therefore the s orbitals of the thallium ions must become polarized onto the DCNQI stacks.[20]

Copper Salts[6]

All DCNQI copper salts are three-dimensional metallic conductors with $\sigma = 100-1000$ Scm^{-1} at ambient temperature. At lower temperatures, however, they split into two groups: group M (metallic conductivity down to lowest temperatures without phase transition as shown in Figure 3), group M $\rightarrow$ I [on cooling metallic conductivity breaks down between 210 and 160 K at a sharp phase transition (Peierls transformation)[38] to an insulating state (Figure 4)]. Four-point wiring of the very thin needles of [2-I,5-Me-ODCNQI]$_2$Cu was not possible, although since the ESR signal is totally broadened down to 0.4 K, this salt must definitely belong to group M (Figure 3).
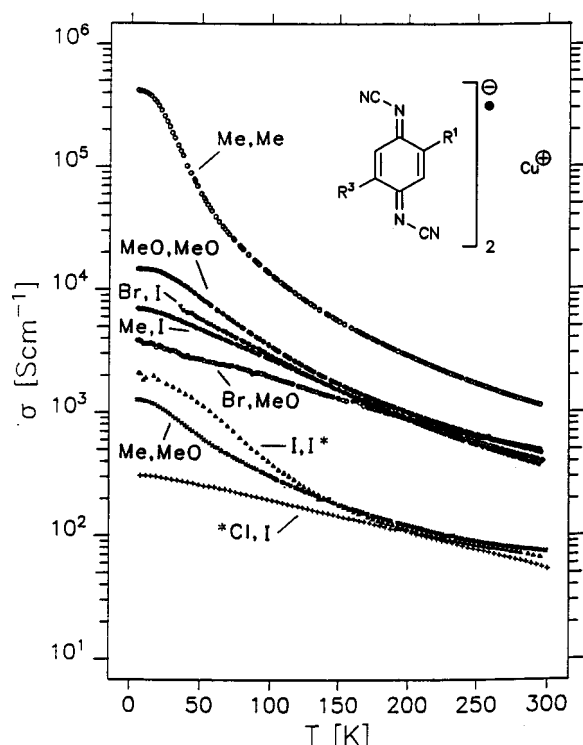
Figure 3. Temperature-dependent conductivities of DCNQI−Cu salts (group M)

The substituent dependence of this different behaviour, as well as the substituent-dependent temperature of the phase transitions, has been thoroughly discussed.[6,8,33] [2,5-Me$_2$DCNQI]$_2$Cu displays the highest conductivity (500000 Scm^{-1}) at 0.4 K, but is a borderline case of group M; under pressure[44] or on deuteration[33,34] it switches to group M $\rightarrow$ I (vide infra).

Temperature-Dependent Conductivity of Alloys of DCNQI−Cu Salts

As already discussed, most alloys of copper salts with two or three different DCNQI ligands display high metallic conductivities (see Table 5). Compared to the situation pictured in Figures 3 and 4 conductivity/temperature correlations of the following alloys are therefore of special inter-
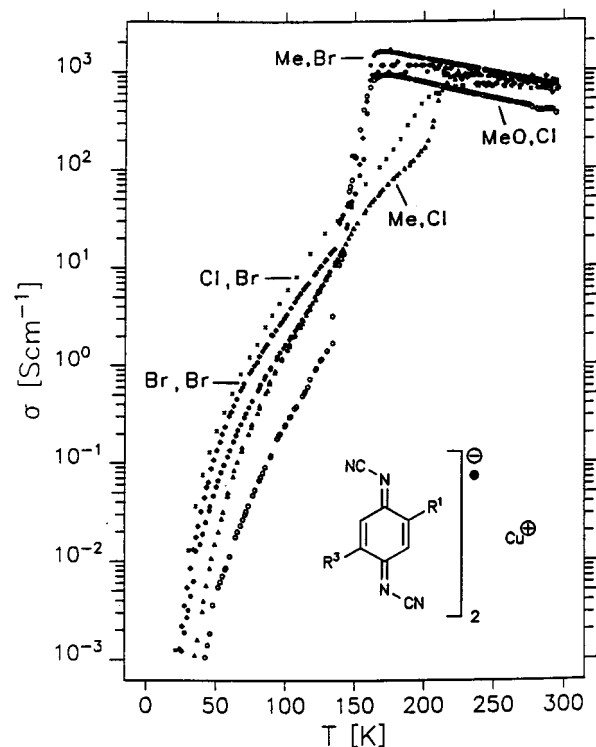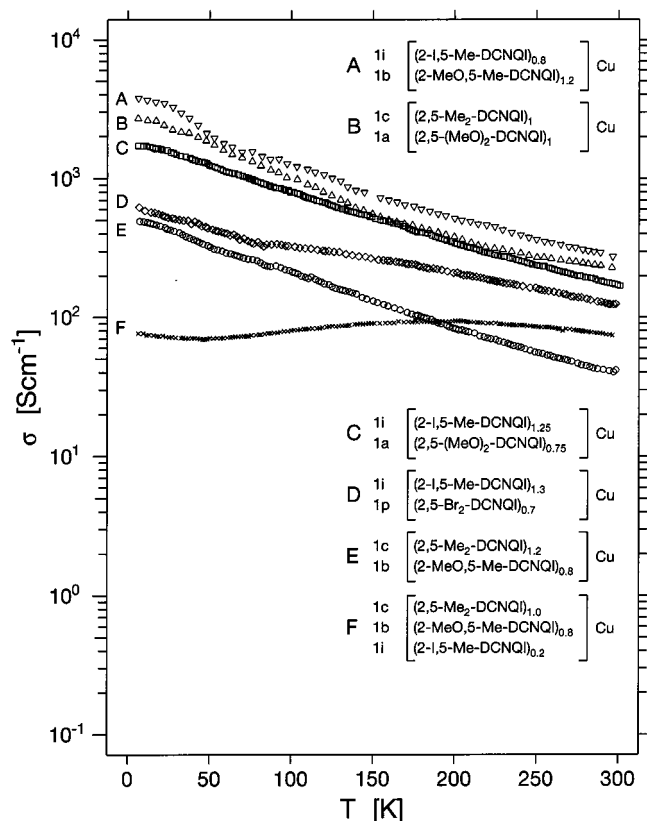

Figure 4. Temperature-dependent conductivities of DCNQI−Cu salts (group M $\rightarrow$ I)

est: (1) all ligands from group M; (2) one ligand group from M, the other from group M $\rightarrow$ I; (3) all ligands from group M $\rightarrow$ I at constant and varying ratios of acceptors.

For alloys grown on a copper wire from solutions of the acceptors in acetonitrile with ratios close to 1:1 (Table 5) temperature-dependent conductivities were registered and are collected in Figures 5 and 6. In Figure 5 the similarity of the ascending slopes of curves A−E is remarkable. Curves A and C show a pattern which is expected from that of the pure DCNQI−Cu salts of Figure 3. In the case of curves B and E the strong increase in conductivity of [2,5-Me$_2$DCNQI]$_2$Cu (Figure 3) is suppressed in its alloys. Curve D represents the first case in which the M $\rightarrow$ I transition of one component ([2,5-Br$_2$DCNQI]$_2$Cu, Figure 4) is suppressed by alloying it with a group-M partner. The slight dip at ca. 80 K may reflect the suppressed M $\rightarrow$ I transition.

Another surprise comes from curve F which marks the *nearly constant conductivity over a range of 5−300 K (!)* of this ternary alloy. From the metallic behaviour of all three single components (Figure 3) an increase of conductivity as in curves A−E of Figure 5 was at least anticipated. This unprecedented behaviour demonstrates *the high potential of ligand alloying by producing temperature-independent conducting materials.*

The alloys listed in Figure 6 (except D) all belong to group M $\rightarrow$ I, albeit with strongly differing phase transitions. Curves B, C, and D resemble those for metal-like semiconductors (Figure 4). This behaviour cannot be simply connected to the fact that these alloys contain a group-M and a group-M $\rightarrow$ I ligand (A, B, C and E); only alloys
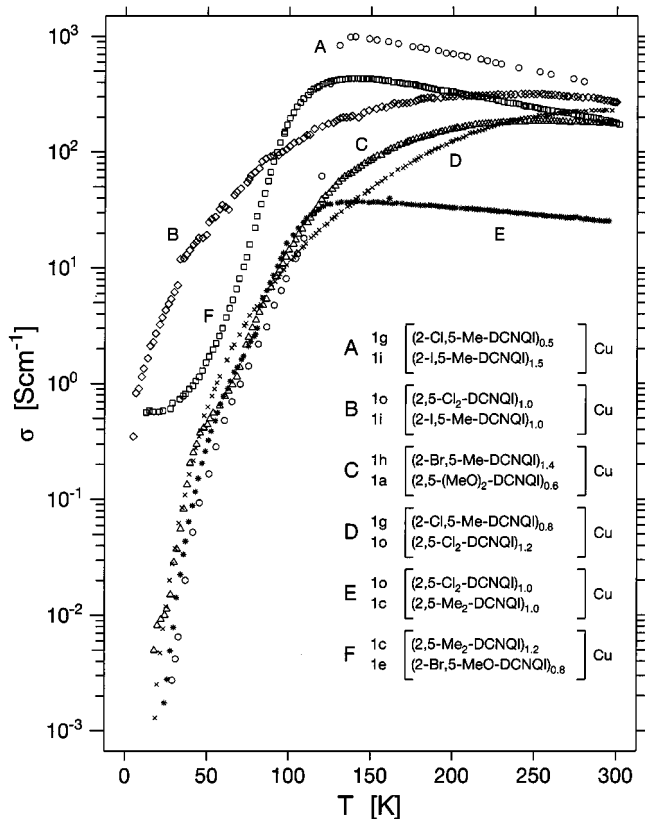
Figures 5. Temperature-dependent conductivities of alloys [2-X,5-Y-DCNQI]$_m$(2-W,5-Z-DCNQI)$_n$−Cu grown from the acceptors on a copper wire; for m and n see Table 5; group-M alloys

Figures 6. Temperature-dependent conductivities of alloys [2-X,5-Y-DCNQI]$_m$(2-W,5-Z-DCNQI)$_n$−Cu grown from the acceptors on a copper wire; for m and n see Table 5; group-M → I alloys

A and E suffer from a sharp phase transition. In addition, *the binary alloy formed from two group-M → I ligands (D) with sharp phase transitions (Figure 4) has lost this feature completely.*

The shape of curve F was not expected at all because both ligands of the alloy belong to group M (Figure 3). Obviously the borderline ligand 2,5-Me$_2$DCNQI cannot keep its group-M properties. The levelling off of curve F at < 30 K is unusual and may be connected to the reentry phenomenon of [2,5-Me$_2$DCNQI]$_2$Cu observed under pressure[28] or by alloying with its deuterated counterpart[33][34] (vide infra).

An alloy composed of the borderline group-M salt and a typical group-M → I salt, [(2,5-Me$_2$DCNQI)$_m$(2-Br,5-MeDCNQI)$_n$]$_2$Cu was also investigated (Figure 7). With the small fraction $n = 0.025$ (curve B) the metallic behaviour is principally retained ($m = 0.975$). However, the inflection between 100 and 50 K marks a phase transition which is reversed at lower temperatures ("reentrance phenomenon", vide infra). However, for $n = 0.37$ (curve C) at ca. 90 K a sharp M → I transition occurs typical for $n = 1$ (curve F, M → I at ca. 170 K) but at much lower temperatures (ca. 90 K). Interestingly, with $n = 0.63$ and $n = 0.88$ (curves D and E) this sharp phase transition disappears and a pattern is observed which resembles that of metal-like semiconductors. Independent investigations of the same alloyed DCNQI copper salt[23] are consistent with these results.

The last series of alloys studied comprised one "normal" group-M acceptor and one group-M → I acceptor [(2-I,5-MeDCNQI)$_m$(2-Br,5-MeDCNQI)$_n$]$_2$Cu (Figure 8).

In this alloy the type of metallic conductivity observed for $m = 1$ ($n = 0$, curve A) is preserved for $n = 0.42$ (curve B) and even for $n = 0.60$ (curve C) although the latter shows signs of a phase transformation. With a slightly higher concentration of the group-M → I component, $n = 0.69$ (curve D), a sharp phase transition occurs at ca. 110 K which keeps its pattern but moves closer to that of pure $n = 1$ (curve G) with $n = 0.83$ and $n = 0.92$ (curves E and F).

The rather low sensitivity of [2-I,5-MeDCNQI]$_2$Cu to doping with a second partner results from the disorder in the crystal lattice caused by the large iodine and the small methyl substituents. The bromine substituents in 2-Br,5-MeDCNQI may possibly just occupy the positions of the iodine substituent in the first ligand.

Temperature-Dependent Conductivities in Deuterated [2,5-Me$_2$DCNQI]$_2$Cu Alloys

The most remarkable effects observed for some of these alloys have already been discussed in detail.[33,45,46] For comparison with the alloys described above some features
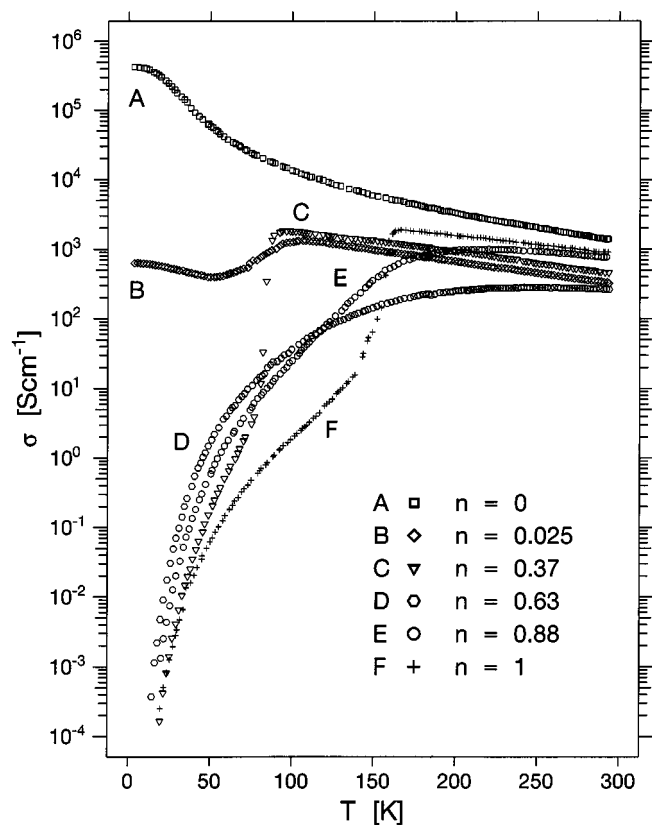
Figure 7. Temperature-dependent conductivities of alloys [(2,5-Me$_2$DCNQI)$_m$(2-Br,5-MeDCNQI)$_n$]$_2$Cu
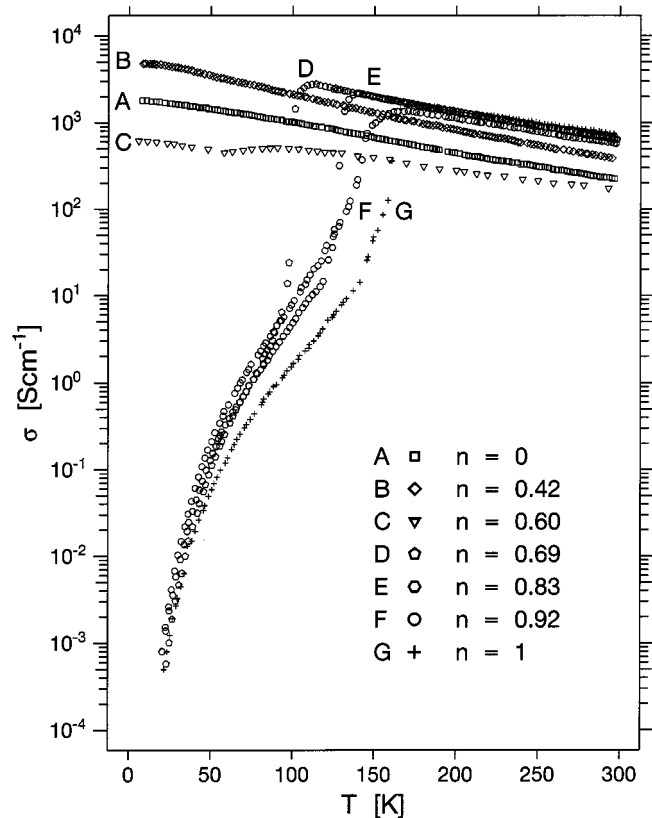
Figure 8. Temperature-dependent conductivities of alloys [(2-I,5-MeDCNQI)$_m$(2-Br,5-MeDCNQI)$_n$]Cu

of {(2,5-Me$_2$DCNQI)$_m$[2,5-(CD$_3$)$_2$DCNQI]$_n$}Cu alloys ("H$_8$/D$_6$") should be also be addressed here.

As seen in Figure 9, the metallic behaviour of "H$_8$" at temperatures down to 0.4 K is lost in "D$_8$". In this case, a sharp phase transition is observed at 73 K, where the conductivity drops by the order of 10^7-10^9.
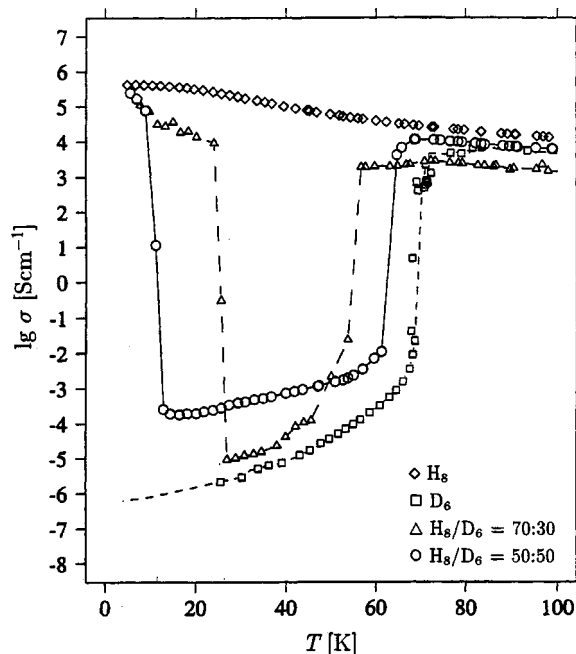

Figure 9. Temperature-dependent conductivities of [2,5-Me$_2$DCN-QI]$_2$Cu (H$_8$) and [2,5-CD$_3$DCNQI]$_2$Cu (D$_6$) together with their alloys

On cooling, alloys with H$_8$/D$_6$ = 70:30 and 50:50 show similar conductivities and phase transitions. However, at lower temperatures (25 K and 12 K, respectively) reentrance into the starting phase occurs with complete regeneration of the high conductivities. This process is connected to a strong hysteresis as shown for H$_8$/D$_6$ = 70:30 in Figure 10a. Using this phenomenon a very sensitive pressure/light-triggered switch can be designed.[46] Outside the highly conducting state the extremely broad ESR signal narrows sufficiently to become visible (Figure 10b and c).

All the results presented in this section clearly demonstrate that alloying DCNQI copper salts provides a powerful tool for manipulating the temperature dependence of conductivity within an unprecedented broad range.

Crystal Structures of DCNQI Metal Salts

All published structures of DCNQI salts with monovalent cations exist in the same 2:1 stoichiometry. The space group in which the salts crystallize depends entirely on the cation and not on the substituent (Scheme 1) and may be either $I4_1/a$ or the closely related space group $P4/n$ and $C2/c$ (or $I2/a$, respectively).

The structures of all radical-anion salts listed in Tables 2−4 also fit completely into this scheme. Some of these structures have already been published.
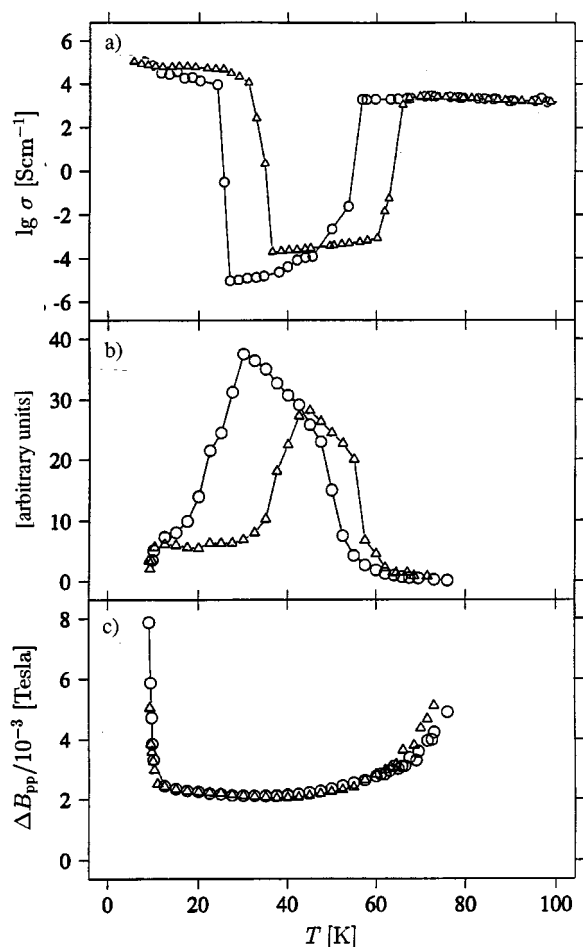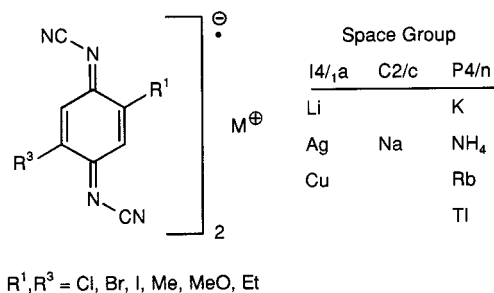
Figure 10. Alloy "H_8/D_6" = 70:30; temperature dependence of a) conductivity, b) ESR intensity, c) ESR line width; O = cooling; Δ = warming

Scheme 1. Space groups for radical-anion salts [2-X,5-Y-DCNQI]$_2$M

Thallium(+1) salts resemble both silver and potassium salts. Due to the large ionic radius of this cation (K^+ = 133 pm, Tl^+ = 147 pm) the radical-anion salts (**1c**)$_2$Tl, (**1h**)$_2$Tl and (**1i**)$_2$Tl (Table 4) adopt space group $P4/n$. The special features of [2,5-Me$_2$DCNQI]$_2$Tl [(**1c**)$_2$Tl] have already been discussed.[20] Its structural data will be included here only for comparison with the isomophic structure of [2,5-(Me-

O)$_2$DCNQI]$_2$Rb[48] of the same space group and with [2-Br,5-IDCNQI]$_2$Cu[48] of type $I4_1/a$ (Scheme 2).

Scheme 2 reveals the close relationship between the two space groups. The very similar bond lengths within the DCNQI ligands are especially remarkable, in spite of their different substituent pattern in these three examples.

The coordination angle α = 122.5° in the c direction of the somewhat flattened tetrahedron in [2-Br,5-IDCNQI]$_2$Cu is below the limiting angle for phase transition and therefore guarantees metallic conductivity down to low temperatures.[33] The lengths of the four N−Cu bonds are equal (198.7 pm) whereas the cubic coordination in the rubidium− and thallium−DCNQIs involves two sets with four DCNQIs of different M−NC bond lengths (Rb: 303.3 and 310.9 ppm; Tl: 293.8 and 318.1 ppm).

The ligands are arranged in skewed stacks with the favourable "ring-over-bond" arrangement that is typical for these radical-anion salts and which provides maximum π-orbital overlap for electron transfer. As is seen in Figure 11, even the bent methoxy groups in [2,5-(MeO)$_2$DCNQI]$_2$Rb are coplanar with the π system.

A Comparison of Structural Information from X-ray Single-Crystal and Powder-Diffraction Data

Although DCQNI−metal salts can easily be prepared as microcrystalline solids, suitable crystals for single-crystal X-ray analysis cannot, so far, be obtained for all salts. Structural information from X-ray powder diagrams would therefore be most welcome. In 1967, H. M. Rietveld derived a mathematical procedure for successfully refining crystal structures from neutron powder-diffraction data.[47] This method, which in the beginning was mostly employed for metal or inorganic crystals with small unit cells, has now been extended to X-ray diffraction data of not only inorganic but also organic compounds. T. Bauer[48] was one of the first to compare systematically crystal-structure refinements of organic compounds based on X-ray single-crystal and powder-diffraction data. These results are reported in this paper.

Since DCNQI radical-anion salts crystallize as isotypic compounds in space group $I4_1/a$ or related groups they represent good examples for a Rietveld treatment even though the highly ordered microcrystals can give rise to preferred orientation in the powder sample, an effect which has to be reduced by special sample preparation or corrected for during refinement. To test the reliability of this simple method, the corresponding single-crystal X-ray data of nine of these DCNQI copper salts were used as standards for comparison. Relevant parameters of single-crystal data and their deviations measured by powder diffraction are given in Table 6 (the data themselves are collected in Tables 2 and 3 of the Supporting Information).

Entries 1−5 clearly demonstrate that the cell parameters, as well as the angles around the coordination centers (Cu), and also the distances between the π planes are obtained

*I*4₁/a
Distorted tetrahedral coordination
at M......N ≡ C–R
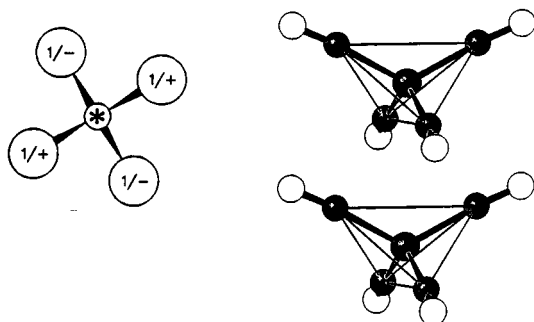
*P*4/ₙ
Cubic coordination with two
different M......N ≡ C–R
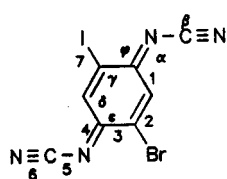distances
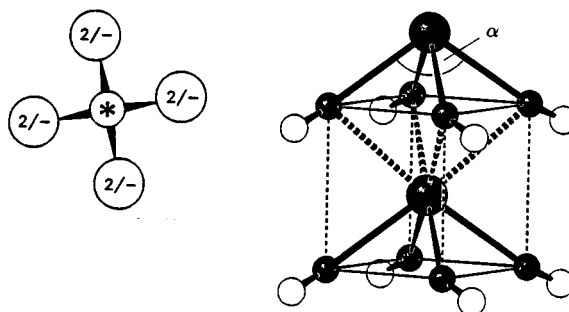
$I4_1/a$
KZ = 4, M = Cu, Li, Ag
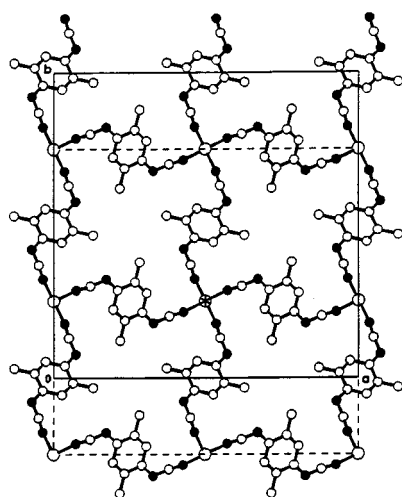
$P4/n$
KZ = 8, M = K, Rb, Tl
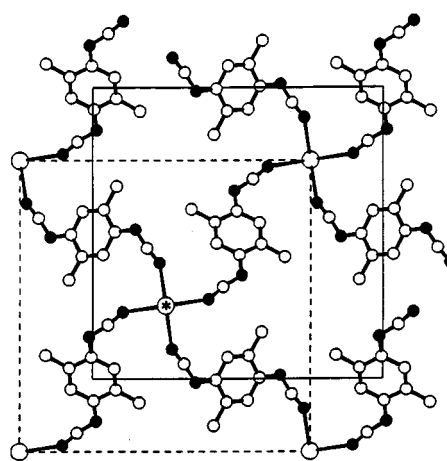
a,b-projection

a,b-projection along c [001]
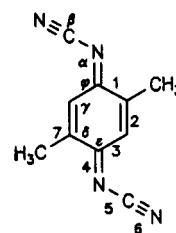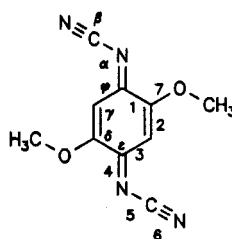
[2-Br,5-I-DCNQI]₂Cu	
Bond Length [pm]	Angle [°]
1 = 144.6(5)	α = 120.6(4)
2 = 135.0(6)	β = 173.0(5)
3 = 143.3(6)	γ = 120.8(4)
4 = 132.3(6)	δ = 118.0(4)
5 = 132.7(5)	ε = 121.7(3)
6 = 116.0(5)	φ = 117.5(4)
7 = 200.8(4)	

[2,5-(MeO)₂-DCNQI]₂Rb	
Bond Length [pm]	Angle [°]
1 = 142.6(3)	α = 120.1(2)
2 = 135.4(3)	β = 172.4(3)
3 = 146.2(3)	γ = 120.4(2)
4 = 132.6(3)	δ = 121.3(2)
5 = 131.7(3)	ε = 121.3(2)
6 = 115.0(4)	φ = 117.6(2)
7 = 134.0(3)	

[2,5-Me₂-DCNQI]₂Tl	
Bond Length [pm]	Angle [°]
1 = 144.1(7)	α = 121.7(4)
2 = 135.2(7)	β = 172.0(6)
3 = 144.6(7)	γ = 116.8(4)
4 = 132.6(6)	δ = 118.6(4)
5 = 132.1(8)	ε = 121.7(5)
6 = 115.0(7)	φ = 119.8(5)
7 = 149.9(8)	

Scheme 2. Structural arrangements of radical-anion salts [2-X,5-Y-DCNQI]₂M in space groups *I*4₁/*a* and *P*4/*n* and typical parameters of the ligands
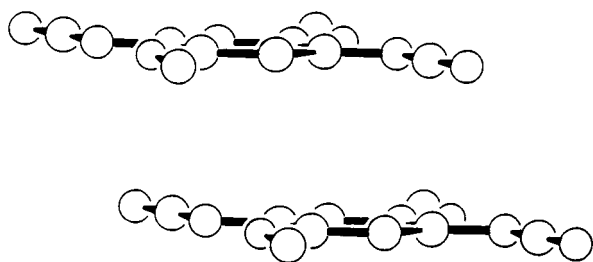
Figure 11. Side view of two ligands in the stacks of [(2,5-Me₂DCN-QI)DCNQI]₂Br

Table 6. Precision of powder-diffraction data after Rietveld analysis compared to single-crystal X-ray data (± 0.3 to 1.0 pm, ± 0.4 to 0.8°) for radical-anion copper salts from **1a**, **1c**, **1g**, **1h**, **1i**, **1k**, **1l**, **1o**, **1p**; unit-cell data (space group $I4_1/a$) and coordination geometries (entries 1−5); bond lengths (BL) and angles of the DCNQI ligands (entries 6−14)

	Range of data from single crystals	Maximal deviation by powder data
1	a axis 2162−2252 pm	−3 to + 1 pm
2	c axis 381−411 pm	−0.3 to 0.2 pm
3	∠ α 126−138°	−0.5 to 0.5°
4	∠ θ 155−178°	−0.4 to +0.3°[a]
5	$d_{\Phi-\Phi}$ 314−321 pm	0 to +3 pm
6	d_{CN-Cu} 196−198 pm	−10 to 5 pm
7	BLa 138−145 pm	−2 to 10 pm[b]
8	BLb 133−135 pm	−5 to 7 pm
9	BLc 143−145 pm	−11 to +9 pm
10	BLd 133−134 pm	−5 to 8 pm
11	BLe 130−132 pm	−9 to + 12 pm
12	BLf 115−116 pm	−10 to 12 pm
13	∠ β CNC 120−121°	−9° to +6°
14	∠ NCN 171°	−14 to 0 pm

[a] Only for **10**: +10°. − [b] Only for **1**: +28 pm.

from powder diffraction with excellent accuracy. Compared to single-crystal data they stay well within the range of error.

However, the powder data connected to the ligand (various bond lengths and angles, entries 6−14) are much less accurate. They are still useful to picture the geometry around the ligand but not precise enough to compare the rather subtle effects of the 2,5-substituents in DCNQIs.

The same situation was found for various non copper salts (M = Li, Na, K, Rb, Tl, Ag; details see Table 4 of Supporting Information).

In Table 7 unit-cell data from powder diffraction are listed for those DCNQI radical salts where single crystals were not available. They have to be considered as highly

reliable and therefore can be discussed safely like the corresponding data by single-crystal X-ray analysis.

Since further improvements in powder-diffraction techniques and evaluation of data have been already achieved in the meantime, this method is expected to gain increasing importance for organic microcrystalline solids.

Conclusions

The broad range of investigations on DCNQI derivatives presented in this paper reports on our concluding efforts in this field. Backed by the experiences gained in the last 12 years we succeeded to answer the questions from which we started in this paper in the following way.

1. In addition to the already successfully tested substituent pattern in 2-X,5-Y-DCNQIs the new substituent pairs in **1d** (Cl/OMe), **1e** (Br/OMe), **1f** (I/OMe), **1j** (Cl/I), **1k** (Br/I), **1l** (I/I) all form CT complexes with TTF (σ ≈ $10^{-1}−10^{-3}$ Scm⁻¹, cf. Table 1) despite the strong increase in size of the halogen substituent. Even one CF₃ group is tolerated [**1m** (OMe/CF₃); **1n** (Me/CF₃)] despite its size and strong electron attraction.

The new anion radical salts all exhibit the stoichiometry [2-X,5-Y-DCNQI]₂M with M = Li, Na, K, NH₄, Rb, Tl, Cu, and Ag prepared by proved methods. With respect to the CF₃ substituent only with **1n** (Me/CF₃) a copper salt deposited. Powder conductivities similar to former ones were found in the usual range ($10^{-1}−10^{-3}$ Scm⁻¹).

2. In some cases the quality of single crystals prepared by electrocrystallization could be improved by partly rhythmic reversal of the redox process. This new method may be of general importance.

3. Much effort was devoted to prepare alloyed DCNQI radical copper salts from two or three differing ligands. The ratio of the DCNQIs in solution is connected to that in the solid radical salt in a nonlinear way (Figure 1). The composition of the alloy surprisingly is hardly determined by the redox potentials of the two DCNQIs but rather by their velocity to form solid radical salts. Since their high conductivities at ambient temperature resemble those of the corresponding DCNQI copper salts with only one type of ligand, the important space group $I4_1/a$ obviously is preserved. These experiments clearly demonstrate that a wealth of alloyed DCNQI copper salts can be designed. This variation offers an approach to organic metals with rather unexpected and partly unprecedent patterns of temperature-dependent conductivity (vide infra).

4. Investigation of the temperature-dependent conductivities of various alloyed DCNQI copper salts produced remarkable, unexpected effects. Instead of duplicating the pattern of the single components incorporated into the alloys, new patterns evolved: Metal insulation phase transitions may be induced, excluded or shifted to a different temperature range. Most remarkably even a temperature-independent conductivity between 5 and 300 K can be achieved (Figure 5). On the other hand the alloyed copper salt from 2,5-Me₂DCNQI and its deuterated counterpart

Table. 7. Unit-cell data of various salts [2-X, 5-Y-DCNQI]$_2$M observed from powder-diffraction data refined by Rietveld analysis

DCNQI	R^1/R^3	M	Space group	a axis [pm]	c axis [pm]	PC−PDF[49]
1a	OMe/OMe	Na	I2/a[a]	2422.9(5) b = 379.8(1)	2280.1(3) β = 91.2(1)°	41−1885
1b	Me/OMe	Rb	P4/n	1668.3(2)	383.50(8)	41−1783
1c	Me/Me	Li	I4$_1$/a	2183.4(4)	385.3(1)[b]	40−1624
	Me/Me	NH$_4$	P4/n	1634.9(2)	385.14(9)	41−1784
	Me/Me	Rb	P4/n	1611.9(6)	382.78(4)	40−1987
1h	Me/Br	Li	I4$_1$/a	2190.6(2)	387.00(6)	40−1979
1i	I/Me	Li	I4$_1$/a	2294.7(1)	395.0(1)	40−1990

[a] Different but symmetrically equivalent setting of the unit cell see ref.[27] − [b] Structure not refined.

on cooling undergoes sharp phase transition with loss of conductivity of 10^7 to 10^8 Scm^{-1} which is restored at even lower temperatures (Figure 9). Because a rather broad hysteresis between heating and cooling is involved this phenomenon can be exploited for a very sensitive pressure/light-triggered switch (Figure 10).

These two extreme patterns qualify ligand alloying of DCNQI copper salts as a powerful tool for the design of highly conducting materials with a definite temperature profile.

5. Radical-anion salts of the type [2-X,5-Y-DCNQI]$_2$M with X,Y = MeO, Me, Cl, Br, I and M$^+$ = Li, Na, K, NH$_4$, Rb, C, M, Ag, Cu prefer the space group I4$_1$/a or a closely related one. Therefore only in this type of organic metals relations between the individual electric properties and very subtle changes of the crystal lattice can be evaluated, provided single crystals for X-ray analysis are at hand. Since often only microcrystalline material is available extension to the evaluation of powder diagrams by the so-called Rietveld analysis is most welcome. This method, so far not employed to organic metals, yields excellent cell data of various DCNQI copper salts but less precise values for the geometries of the ligands.

Experimental Section

General: Melting points of the DCNQI/TTF complexes and the DCNQI radical-anion salts could not be determined with a Kofler microscope but had to be determined by differential thermoanalysis (DTA, Du Pont de Nemours Thermal Analyser TA 990). − IR spectra: Perkin Elmer 1420 and Nicolet 5 DXC FT-IR spectrometer. − Conductivities of microcrystalline solids were measured in a quartz capillary by compressing the powder with the two electrodes until the first cracks were seen. Single crystals were measured by the standard 4-point method. Solvents were purified and dried according to standard methods. Data from crystal-structure analyses: see Tables 8 and 9.

Neutron-Activation Analysis of Bromine and Copper (Table 6): The copper and bromine contents of the substances were determined by neutron-activation analysis (NAA). As reference nuclides ^{64}Cu ($t_{1/2}$ = 12.700 h) was used for copper and ^{82}Br ($t_{1/2}$ = 35.34 h) for bromine. Samples and standards were packed in quartz ampoules (Suprasil AN, Heraeus Quarzschmelze GmbH, Hanau) which had been cleaned before use. The sample mass per analysis was between 0.5 and 4 mg. Copper standard: copper(II) oxide granulated for analysis (E. Merck, Darmstadt), weighed in quantities betweeen

1.6 and 4.5 mg. Bromine standard: 50 µL of a KBrO$_3$ solution with p_{Br} = 2.664 g/l (Fixanal®, Riedel-de Haen, Seelze) was dried in a quartz ampoule (desiccator) → m_{Br} = 133.2 µg. Of the sealed ampoules, sets consisting of three samples, including a copper standard and a bromine standard were packed in aluminium foil and irradiated in the Forschungsreaktor München at xxx$_{th}$ Ø$_{th}$ = 1.3 × 10^{13} cm^{-2}s^{-1}. Irradiation time = 15 min. After a waiting time (t_w) between 30 and 50 h the samples and standards were measured in the ampoules which had been cleaned outside.[50] − Counting equipment: 130-cm^3 intrinsic coaxial Ge detector, 1.9 keV resolution and 27% relative efficiency (both for the 1332.47-keV γ-line of ^{60}Co), main amplifier Silena model 7611, ADC Silena model 7423 UHS, memory buffer module Silena 7329−16K, personal computer AT/03/CO. For the evaluation of the γ spectra, emulation software mmb3 (Silena) was used. The ampoules were positioned with their axis parallel to the detector surface at a distance of 20 to 50 cm. The counting time was usually 2 h.

As a reference line for ^{64}Cu in most cases the 511-keV line was used (annihilation radiation of β$^+$ of ^{64}Cu). The 1345.9-keV γ-line (I_{rel} = 0.6%) was taken as the reference line if the 1368.6-keV γ-line of ^{24}Na was detected because ^{24}Na causes 511-keV radiation, too (a consequence of the pair production of the ^{24}Na γ-rays of 1368.6 keV and of 2754.1 keV). In addition, a contribution to the 511-keV line was taken into consideration by the pair ^{80m}Br (I.T.) ^{80}Br which is generated in parallel with ^{82}Br from bromine by neutron irradiation. ^{80}Br emits β$^+$ (2.6%). Its $t_{1/2}$ is only 17.6 min, but the $t_{1/2}$ of ^{80}Br is 4.2 h. Estimations by both calculation and measurement of bromine standards showed that after the above-mentioned t_w a contribution to the 511-keV line caused by ^{80}Br was either not detectable or negligibly small. For ^{82}Br its 776.49-keV γ-line (I_{rel} = 83%) was used as a reference.

DCNQI/TTF Complexes. − General Procedure 1 (GP1): Under nitrogen a concentrated solution of TTF in MeCN or dichloromethane (DCM) was added dropwise to a concentrated solution of the DCNQI in MeCN (20−80°C) or DCM. From the dark green to black solution the black microcrystalline charge-transfer complex separated within 1 min to 10 h. After cooling (0 to 10°C) of the mixture overnight, the solid was separated, washed with solvent and pentane and dried over silica gel (see Table 1).

2-Chloro-N,N′-dicyano-5-methoxy-1,4-benzoquinonediimine/Tetrathiafulvalene (1:1, 1d/TTF): TTF (30.4 mg, 100 µmol) in MeCN (1 mL); **1d** (22.1 mg, 100 µmol) in MeCN (3 mL, 60°). **1d**/TTF (37.0 mg, 93%), m.p. 155°C.− IR (KBr): ṽ = 4000−600 cm^{-1} total absorption. − C$_{15}$H$_9$ClN$_4$OS$_4$ (424.7): calcd. C 42.42, H 2.14, N 13.30; found C 40.33, H 2.05, N 12.27.

2-Bromo-N,N′-dicyano-5-methoxy-1,4-benzoquinone/Tetrathiafulvalene (1:1; 1e/TTF): TTF (40.8 mg, 200 µmol) in MeCN (2 mL);

Table 8. Single-crystal X-ray data

Compound	[1a]₂Rb[48]	[1c]₂Tl[20]	[1k]₂Cu[48]
Empirical formula	$C_{20}H_{16}N_8O_4Rb$	$C_{20}H_{16}N_8Tl$	$C_{16}H_4Br_2CuI_2N_8$
Molecular mass	517.87	572.77	785.43
a [pm]	1697.9(4)	1604.3(3)	2165.3(6)
c [pm]	384.0(2)	380.9(1)	402.3(2)
V [pm³]	$1107(1) \times 10^6$	$980(1) \times 10^6$	$1886(1) \times 10^6$
Z	2	2	4
d(calcd.) [g cm⁻³]	1.55	1.94	2.77
Space group	$P4/n$	$P4/n$	$I4_1/a$
Diffractometer	Nonius	CAD-4	CAD-4
Radiation		Mo-K_α	
Monochromator		graphite	
Crystal size [mm]	$0.09 \times 0.12 \times 0.9$	$0.03 \times 0.03 \times 0.11$	$0.03 \times 0.05 \times 0.9$
Data collection mode		ω-2θ	
θ range [°]	1−25	1−20	2−30
Reciprocal lattice segment	$h = 0 \rightarrow 20$	$h = 0 \rightarrow 14$	$h = 0 \rightarrow 30$
	$k = 0 \rightarrow 20$	$k = -14 \rightarrow 14$	$k = 0 \rightarrow 30$
	$l = 0 \rightarrow 4$	$l = 0 \rightarrow 4$	$l = -5 \rightarrow 5$
No. refl. measd.	1050	933	2692
No. unique refl.	979	456	1371
No. refl. $F_o^2 > 2 \sigma(F_o^2)$	907	430	1186
μ [mm⁻¹]	2.22	8.94	8.65
Absorption correction		Ψ scan	
Solution by		Patterson method	
Method of refinementfull-matrix least-squares, H atoms isotropic			
Data-to-parameter ratio	9.9	5.4	16.9
R, R_w	0.031, 0.041	0.012, 0.014	0.039, 0.044
Weighting scheme		$w = 4 F_o^2/\sigma^2(F_o^2)$	
Largest difference peak	0.6 e/Å³	0.2 e/Å³	1.5 e/Å³
Largest difference hole	0.2 e/Å³	0.2 e/Å	0.4 e/Å³
Program used		SHELX76	

1e (53.0 mmg, 200 μmol) in MeCN (6 mL, 60°C). **1e/TTF** (70.0 mg, 75%), m.p. 160°C. − IR (KBr): ṽ = 4000−600 cm⁻¹ total absorption. − $C_{15}H_9BrN_4OS_4$ (469.4): calcd. C 38.38, H 1.94, N 11.94; found C 38.51, H 1.85, N 11.97.

N,N′-Dicyano-2-iodo-5-methoxy-1,4-benzoquinonediimine/Tetra-thiafulvalene (1:1; 1f/ TTF): TTF (40.8 mg, 200 μmol) in MeCN (15 mL); **1f** (62.0 mg, 200 μmol) in MeCN (5 mL, 80°C). **1f/TTF** (77 mg, 74%), m.p. 122°C (dec.). − IR (KBr): ṽ = 4000−600 cm⁻¹ total absorption. − $C_{15}H_{19}IN_4OS_4$ (516.4): calcd. C 34.89, H 1.76, N 10.85; found C 35.02, H 1.73, N 10.85.

2-Chloro-N,N′-dicyano-5-iodo-1,4-benzoquinonediimine/Tetra-thiafulvalene (1:1; 1j/TTF): TTF (20.4 mg, 100 μmol) in DCM (1 mL); **1j** (31.6 mg, 100 μmol) in DCM (10 mL). **1j/TTF** (40.0 mg, 77%), m.p. 125°C. − IR (KBr): ṽ = 2110 cm⁻¹. − $C_{14}H_6ClIN_4S_4$ (520.6): calcd. C 32.30, H 1.16, N 10.76; found C 32.05, H 1.16, N 10.66.

2-Bromo-N,N′-dicyano-5-iodo-1,4-benzoquinonediimine/Tetra-thiafulvalene (1:1; 1k/TTF): TTF (20.4 mg, 100 μmol) in DCM (1 mL); **1k** (36.1 mg, 100 μmol) in DCM (10 mL). **1k** (44.0 mg, 78%), m.p. 127°C (dec.). − IR (KBr): ṽ = 2110 cm⁻¹. − $C_{14}H_6BrIN_4S_4$ (565.0): calcd. C 29.74, H 1.07, N 9.92; found C 29.18, H 0.74, N 9.60.

N,N′-Dicyano-2,5-diiodo-1,4-benzoquinonediimine/Tetrathia-fulvalene (1:1; 1j/TTF): TTF (20.4 mg, 100 μmol) in DCM (1 mL); **1l** (41.0 mg, 100 μmol) in DCM (20 mL). **1l/TTF** (51.0 mg, 83%), m.p. 152°C (dec.). − IR (KBr): ṽ = 2080 cm⁻¹. − $C_{14}H_6I_2N_4S_4$ (612.3): calcd. C 27.46, H 0.99, N 9.15; found C 27.72, H 0.97, N 9.45.

N,N′-Dicyano-2-methoxy-5-trifluoromethyl-1,4-benzoquino-nediimine/Tetrathiafulvalene (1:1; 1m/TTF): TTF (48.0 mg, 200 μmol) in MeCN (1 mL); **1m** (51.0 mg, 200 μmol) in MeCN (4 mL). **1m/TTF** (93.2 mg, 98%), m.p. 126°C. − IR (KBr): ṽ = 2100 cm⁻¹. − $C_{16}H_9F_3N_4OS_4$ (458.5): calcd. C 41.91, H 1.99, N 12.22, S 27.96; found C 41.79, H 2.26, N 11.92, S 26.85.

N,N′-Dicyano-2-methyl-5-trifluoromethyl-1,4-benzoquinonediimine/ Tetrathiafulvalene (1:1; 1n/TTF): TTF (40.8 mg, 200 μmol) in MeCN (4 mL); **1n** (48.0 mg, 200 μmol) in MeCN (3 mL). **1n/TTF** (80.0 mg, 90%). − $C_{10}H_9F_3N_4S_4$ (442.5): calcd. C 43.43, H 2.05, N 12.66, S 28.98; found C 42.53, H 2.08, N 11.60, S 31.02.

DCNQI Radical-anion Salts from Iodides. − General Procedure 2 (GP2): Under nitrogen a concentrated, degassed and filtered solution of the metal (ammonium) iodide in MeCN was added to a concentrated solution (20−80°C) of the DCNQI in MeCN. The black microcrystalline salt deposited from the dark solution. After cooling, the solid was separated, washed with MeCN and pentane and dried over silica gel (see Table 2).

Bis(N,N′-dicyano-2,5-dimethoxy-1,4-benzoquinonediimine)lithium [(1a)₂Li]: 1a (43.2 mg, 200 μmol) in MeCN (4 mL, 50°C); lithium iodide (54 mg, 400 mmol) in MeCN (2 mL). **(1a)₂Li·H₂O** (40.0 mg, 88%), m.p. 211°C (dec.). − IR (KBr): ṽ = 3400 cm⁻¹ (O−H), 2135 (C≡N). − $[C_{10}H_8N_4O_2]_2Li \cdot H_2O$ (457.4): calcd. C 52.52, H 3.97, N 24.50; found C 52.54, H 3.53, N 24.59.

Bis(N,N′-dicyano-2,5-dimethoxy-1,4-benzoquinonediimine)-potassium [(1a)₂K]: 1a (21.6 mg, 100 μmol) in MeCN (2 mL, 80°C); potassium iodide (33 mg, 200 mmol) in MeCN (5 mL). **(1a)₂K** (44.0 mg, 94%), m.p. 170°C (dec.). − IR (KBr): ṽ = 2150 cm⁻¹ (C≡N). − $[C_{10}H_8N_4O_2]_2K$ (471.5): calcd. C 50.51, H 3.40, N 23.57; found C 50.72, H 3.07, N 24.01.

Bis(N,N′-dicyano-2,5-dimethoxy-1,4-benzoquinonediimine)rubidium [(1a)₂Rb]: 1a (21.6 mg, 100 μmol) in MeCN (2 mL, 80°C); rubid-

Table 9. X-ray powder diffraction: experimental parameters and crystallographic data of the DCNQI copper salts obtained by X-ray powder diffraction and Rietveld analysis; all compounds crystallize in space group $I4_1/a$ with $Z = 4$; wavelengths used were $\lambda_1 = 154.056$ pm and $\lambda_2 = 154.439$ pm[48]

Compound	[DMeDCNQI]$_2$-Cu	[Me,ClDCNQI]$_2$-Cu	[Me,BrDCNQI]$_2$-Cu	[Me,IDCNQI]$_2$-Cu	[DClDCNQI]$_2$-Cu	[Cl,JDCNQI]$_2$-Cu
Empirical formula	C$_{20}$H$_{16}$CuN$_8$	C$_{18}$H$_{10}$Cl$_2$CuN$_8$	C$_{18}$H$_{10}$Br$_2$CuN$_8$	C$_{18}$H$_{10}$CuI$_2$N$_8$	C$_{16}$H$_4$Cl$_4$CuN$_8$	C$_{16}$H$_4$Cl$_2$CuI$_2$N$_8$
a [pm]	2162.8(1)	2168.5(1)	2169.5(2)	2170.7(2)	2164.9(1)	2170.3(1)
c [pm]	388.49(4)	383.49(3)	387.59(4)	398.87(3)	381.69(3)	396.77(3)
V [pm$^3 \cdot 10^6$]	1817	1803	1824	1880	1789	1869
$d_\text{calcd.}$ [g/cm^3]	1.58	1.74	2.05	2.32	1.91	2.48
Sample holder[a]	G1.	G1.	Q.	Q.,M.	G2.	G1.
Step width (2θ) [°]	0.03	0.03	0.03	0.03	0.03	0.03
2 θ range [°]	6.5−102	6−102	7−102	8−95	6−100	7−100
No. observations	3183	3200	3167	2900	3133	3100
No. reflections	487	485	489	425	464	481
No. profile parameters	9	9	9	9	9	9
No. structure parameters	31	34	28	23	26	26
$R_{wp} = [\Sigma w_i(y_{oi} - 1/C \cdot y_{ci})^2/\Sigma w_i y_{oi}^2]^{1/2}$ (%)[b]	15.4	10.6	7.6	6.1	8.4	8.1
$R_p' = [\Sigma(y_{oi} - 1/C \cdot y_{ci})^2/\Sigma(y_{oi} - y_{bi})]$ (%)[b]	19.6	18.6	18.8	27.2	19.5	21.9
$R_B = \Sigma|I_{oi} - 1/C \cdot I_{ci}|\Sigma I_{oi}$ (%)[b]	6.3	5.1	6.0	10.4	5.7	7.6
$R_e = [(N - P)/\Sigma w_i y_{oi}]^{1/2}$ (%)[b]	1.6	1.6	2.3	5.5	2.2	3.5
Isotropic displacement parameters refined	yes	yes	partly	no	no	no

Compound	[Me,MeODCNQI]$_2$Cu	[DMeODCNQI]$_2$Cu	DBrDCNQI]$_2$Cu	[DIDCNQI]$_2$Cu	[I,BrDCNQI]$_2$Cu
Empirical formula	C$_{20}$H$_{16}$CuN$_8$O$_2$	C$_{20}$H$_{16}$CuN$_8$O$_4$	C$_{16}$H$_4$Br$_4$CuN$_8$	C$_{16}$H$_4$CuI$_4$N$_8$	C$_{16}$H$_4$Br$_2$CuI$_2$N$_8$
a [pm]	2219.2(1)	2251.5(1)	2162.5(1)	2172.0(6)	2168.3(1)
c [pm]	387.13(2)	384.35(2)	390.71(2)	411.20(2)	402.50(2)
V [pm$^3 \cdot 10^6$]	1907	1948	1827	1944	1892
$d_\text{calcd.}$ [g/cm^3]	1.62	1.69	2.52	3.01	2.76
Sample holder[a]	G1., M.	G2.	Q.	Q.,M.	Q.
Step width (2θ) [°]	0.02	0.03	0.03	0.03	0.03
2 θ range [°]	6−90	6−95	7−100	7.5−114	6−100
No. observations	4176	2967	3100	3550	3133
No. reflections	392	452	474	658	487
No. profile parameters	9	9	9	9	9
No. structure parameters	29	26	31	23	26
$R_{wp} = [\Sigma w_i(y_{oi} - 1/C \cdot y_{ci})^2/\Sigma w_i y_{oi}^2]^{1/2}$ (%)[b]	6.2	7.2	9.1	6.7	10.3
$R_p' = [\Sigma(y_{oi} - 1/C \cdot y_{ci})^2/\Sigma(y_{oi} - y_{bi})]$ (%)[b]	22.3	23.9	15.3	22.2	16.3
$R_B = \Sigma|I_{oi} - 1/C \cdot I_{ci}|\Sigma I_{oi}$ (%)[b]	6.1	8.3	5.6	9.6	4.7
$R_e = [(N - P)/\Sigma w_i y_{oi}]^{1/2}$ (%)[b]	2.5	3.3	1.9	3.8	2.5
Isotropic displacement parameters refined	no	no	yes	no	no

[a] G1.: glass sample holder with a diameter of 22 mm and a depth of 0.25 mm; Q.: quartz sample holder with a diameter of 20 mm and a depth of 0.05 mm; G2.: glass sample holder with a diameter of 25 mm and a depth of 0.05 mm; M.: mixture with glass powder to decrease effects of preferred orientation. − [b] C: scale factor; y_o,y_c,y_b: observed, calculated and background profile intensities; I_o,I_c: observed and calculated integrated intensities; N: number of statistically independent observations; P: number of variable least-squares parameters; w: weight $= 1/y_o$

ium iodide (31.9 mg, 150 µmol) in MeCN (5 mL, 12 h room temp.). **(1a)$_2$Rb** (15.0 mg, 58%), m.p. 170°C (dec.). − IR (KBr): $\tilde{v} = 2140$ cm^{-1} (C≡N). − [C$_{10}$H$_8$N$_4$O$_2$]$_2$Rb (517.9): calcd. C 46.38, H 3.12, N 21.64; found C 46.60, H 2.95, N 20.95.

Bis(*N*,*N'*-dicyano-2-methoxy-5-methyl-1,4-benzoquinonediimine)lithium [(1b)$_2$Li · 1.8 H$_2$O]: 1b (40.0 mg, 200 µmol) in MeCN (3 mL); lithium iodide (54 mg, 400 µmol) in MeCN (2 mL, −20°C, 12 h). **(1b)$_2$Li · 1.8 H$_2$O** (32.0 mg, 73%), m.p. 64°C (dec.). − IR (KBr): $\tilde{v} = 3400$ cm^{-1} (O−H), 2110 (C≡N). − After 3 d a brown amorphous powder was formed by decomposition. − [C$_{10}$H$_8$N$_4$O]$_2$Li · 1.8 H$_2$O (430.9): calcd. C 54.62, H 4.46, N 25.48; found C 54.64, H 3.50, N 27.50.

Bis(*N*,*N'*-dicyano-2-methoxy-5-methyl-1,4-benzoquinonediimine)sodium [(1b)$_2$Na]: 1b (40.0 mg, 200 µmol) in MeCN (3 mL);

sodium iodide (60 mg, 400 mmol) in MeCN (3 mL, 50 → 20°C, 12 h). **(1b)$_2$Na** (42.0 mg, 100%), m.p. 138°C (dec.). − IR (KBr): $\tilde{v} = 2140$ cm^{-1} (C≡N). − [C$_{10}$H$_8$N$_4$O]$_2$Na (423.4): calcd. C 56.73, H 3.80, N 26.46; found C 56.31, H 3.79, N 25.95.

Bis(*N*,*N'*-dicyano-2-methoxy-5-methyl-1,4-benzoquinonediimine)rubidium [(1b)$_2$Rb]: 1b (20.0 mg, 100 µmol) in MeCN (2 mL, 50°C), rubidium iodide (32 mg, 150 µmol) in MeCN (5 mL, −35°C, 12 h). **(1b)$_2$Rb** (17.0 mg, 70%), m.p. 90°C (dec.). − IR (KBr): $\tilde{v} = 2145$ cm^{-1} (C≡N). − [C$_{10}$H$_8$N$_4$O]$_2$Rb (485.9): calcd. C 49.43, H 3.33, N 23.07; found C 48.98, H 3.00, N 22.23.

Bis(*N*,*N'*-dicyano-2,5-dimethyl-1,4-benzoquinonediimine)ammonium [(1c)$_2$NH$_4$]: 1c (55.3 mg, 300 µmol) in MeCN (5 mL, 60°C); ammonium iodide (73 mg, 500 µmol) in MeCN (10 mL, 60 → 20°C). **(1c)$_2$NH$_4$** (35.0 mg, 40%), m.p. 129°C (dec.). − IR (KBr): $\tilde{v} = 2135$

cm^{-1} (C≡N). − [C$_{10}$H$_8$N$_4$]$_2$NH$_4$ (386.4): calcd. C 62.15, H 5.23, N 32.62; found C 61.81, H 5.30, N 32.75.

Bis(2-chloro-*N*,*N′*-dicyano-5-methoxy-1,4-benzoquinonediimine)lithium [(1d)$_2$Li·H$_2$O]: 1d (44.2 mg, 200 μmol) in MeCN (8 mL); lithium iodide (50 mg, 300 μmol) in MeCN (2 mL, 20 → 0°C, 10 min). (1d)$_2$Li·H$_2$O (26.0 mg, 56%), m.p. 76°C (dec.). − IR (KBr): ṽ = 3400 cm^{-1} (O−H), 2240, 2150 (C≡N). − After 4 d, a brown amorphous powder had formed by decomposition. − [C$_9$H$_5$N$_4$ClO]$_2$Li·H$_2$O (466.2): calcd. C 46.37, H 2.60, N 24.04; found C 46.89, H 3.34, N 23.71.

Bis(2-chloro-*N*,*N′*-dicyano-5-methoxy-1,4-benzoquinonediimine)copper [(1d)$_2$Cu]: 1d (44.1 mg, 200 μmol) in MeCN (8 mL, 50°C); copper(I) iodide (59 mg, 300 μmol) in MeCN (4 mL). (1d)$_2$Cu (48.0 mg, 96%), m.p. 180°C (dec.). − IR (KBr): ṽ = 4000−600 cm^{-1}, total absorption. − [C$_9$H$_5$N$_4$ClO]$_2$Cu (504.8): calcd. C 42.85, H 2.00, N 22.20; found C 42.73, H 1.97, N 22.34.

Bis(2-bromo-*N*,*N′*-dicyano-5-methoxy-1,4-benzoquinonediimine)copper [(1e)$_2$Cu]: 1e (26.5 mg, 100 μmol) in MeCN (6 mL, 60°C); copper(I) iodide (29 mg, 150 μmol) in MeCN (5 mL, → 0°C). (1e)$_2$Cu (29.0 mg, 98%), m.p. 176°C (dec.). − IR (KBr): ṽ = 4000−600 cm^{-1}, total absorption. − [C$_9$H$_5$N$_4$BrO]$_2$Cu (593.8): calcd. C 36.41, H 1.70, N 18.88; found C 36.31, H 1.58, N 18.69.

Bis(*N*,*N′*-dicyano-2-iodo-5-methoxy-1,4-benzoquinone)copper [(1f)$_2$Cu]: 1f (57 mg, 300 μmol) in MeCN (3 mL); copper(I) iodide in MeCN (3 mL). (1f)$_2$Cu (65.0 mg, 47%). − IR (KBr): ṽ = 4000−600 cm^{-1}, total absorption. − C$_{18}$H$_{10}$CuI$_2$N$_8$O$_2$ (687.7): calcd. C 31.44, H 1.47, N 16.29; found C 30.60, H 1.37, N 15.81.

Bis(2-bromo-*N*,*N′*-dicyano-5-methyl-1,4-benzoquinonediimine)-ammonium [(1h)$_2$NH$_4$]: 1h (99.6 mg, 400 μmol) in MeCN (5 mL, 60°C); ammonium iodide (87 mg, 600 μmol) in MeCN (10 mL, → 0°C). (1h)$_2$NH$_4$ (87.0 mg, 85%), m.p. 134°C (dec.). − IR (KBr): ṽ = 2145 cm^{-1} (C≡N). − [C$_9$H$_5$N$_4$Br]$_2$NH$_4$ (516.2): C 41.88, H 2.74, N 24.43; found C 41.52, H 2.64, N 23.57.

Bis(*N*,*N′*-dicyano-2-iodo-5-methyl-1,4-benzoquinonediimine)-ammonium [(1i)$_2$NH$_4$]: 1i (119 mg, 400 μmol) in MeCN (6 mL, 60°C); ammonium iodide (87 mg, 600 μmol) in MeCN (10 mL; → 10°C, 1 h). (1e)$_2$Cu (93.0 mg, 77%), m.p. 134°C (dec.). − IR (KBr): ṽ = 2140 cm^{-1} (C≡N). − [C$_9$H$_5$N$_4$I]$_2$NH$_4$ (610.2): calcd. C 35.43, H 2.31, N 20.66; found C 35.85, H 2.44, N 19.85.

Bis(2-chloro-*N*,*N′*-dicyano-5-iodo-1,4-benzoquinonediimine)copper [(1j)$_2$Cu]: 1j (63.3 mg, 200 μmol) in MeCN (10 mL); copper(I) iodide (59 mg, 300 μmol) in MeCN (4 mL, → 10°C). (1j)$_2$Cu (50.0 mg, 72%), m.p. 150°C (dec.). − IR (KBr): ṽ = 4000−600 cm^{-1}, total absorption. − [C$_8$H$_2$N$_4$ClI]$_2$Cu (696.5): C 27.59, H 0.58, N 16.08, found: C 27.78, H 0.77, N 16.11.

Bis(2-bromo-*N*,*N′*-dicyano-5-iodo-1,4-benzoquinonediimine)copper [(1k)$_2$Cu]: 1k (90.3 mg, 250 μmol) in MeCN (25 mL); copper(I) iodide (66.5 mg, 350 μmol) in MeCN (5 mL). (1k)$_2$Cu (72.0 mg, 74%), m.p. 164°C (dec.). − IR (KBr): ṽ = 4000−600 cm^{-1}, total absorption. − [C$_8$H$_2$N$_4$BrI]$_2$Cu (785.4): calcd. C 24.46, H 0.51, N 14.27; found C 24.27, H 0.50, N 14.32.

Bis(*N*,*N′*-dicyano-2,5-diiodo-1,4-benzoquinonediimine)copper [(1l)$_2$Cu]: 1l (40.8 mg, 100 μmol) in MeCN (25 mL, 60°C); copper(I) iodide (38 mg, 200 μmol) in MeCN (5 mL, → 20°C). (1l)$_2$Cu (40.0 mg, 91%), m.p. 164°C (dec.). − IR (KBr): ṽ = 4000−600 cm^{-1}, total absorption. − [C$_8$H$_2$N$_4$I$_2$]$_2$Cu (879.4): calcd. C 21.85, H 0.50, N 12.74; found C 21.49, H 0.59, N 12.41.

Bis(*N*,*N′*-dicyano-2-methyl-5-trifluoromethyl-1,4-benzoquinonediimine)copper [(1n)$_2$Cu]: 1n (72 mg, 300 μmol) in MeCN (4 mL); copper(I) iodide (38 mg, 200 μmol) in MeCN (2 mL). (1n)$_2$Cu (50.0

mg, 62%). − IR (KBr): ṽ = 4000−600 cm^{-1}, total absorption. − C$_{20}$H$_{10}$CuF$_6$N$_8$ (539.9): calcd. C 44.49, H 1.87, N 20.76; found C 44.05, H 2.00, N 21.02. − (1n)$_2$Cu was obtained only with the given stoichiometry of the components. The usual ratio 1n/CuI = 300:450 yielded a different black amorphous compound with a 7:5 stoichiometry, a distinct IR spectrum and σ$_p$ = 2 × 10^{-7} Scm^{-1}, m.p. 168°C (dec.). − IR (KBr): ṽ = 2130 cm^{-1} (C≡N), 1580 (C=N). − C$_{70}$H$_{35}$Cu$_5$F$_{21}$N$_{28}$ (1984.9): calcd. C 42.36, H 1.78, N 19.76; found C 41.82, H 2.23, N 20.05.

DCNQI Radical-Anion Salts Grown on Silver or Copper Wires. − General Procedure 3 (GP3): A silver wire (diameter 0.3 mm) was flattened, polished and treated with toluene and acetonitrile. This wire was immersed 1−2 cm deep into a degassed solution of silver nitrate (100 μmol) and DCNQI 1 (100 μmol) in 8 mL of acetonitrile. After 3−10 d, the solution became colourless and from the silver wire black, shiny needles (1−20 mm) were harvested, washed with MeCN and pentane and dried over silica gel. The same procedure was followed with a copper wire (diameter = 1 mm, cleaned with 2 M HCl/3% H$_2$O$_2$, polished and treated with MeCN. The MeCN solution (10 mL) contained DCNQI 1 (100 μmol) and copper(II) bromide (100 μmol). Analytical data are collected in Table 10, and yields and conductivities in Table 3.

Table 10. Analytical data for DCNQI salts grown on a silver and copper wire

No.	m.p. [°C]	ṽ(C≡N) [$^{-1}$]	Elemental analysis[a]		
			C	H	N
(1c)$_2$Ag	173	2165	50.43	3.39	23.53
			49.75	3.30	22.87
(1d)$_2$Cu	180	[b]	42.82	2.00	22.20
			43.04	1.99	22.48
(1e)$_2$Cu	154	[b]	36.41	1.70	18.86
			36.25	1.65	18.54
(1h)$_2$Ag	162	2140	35.75	1.67	18.49
			34.89	1.28	17.74
(1i)$_2$Ag	159	2170	30.88	1.44	16.01
		2140	31.40	1.32	15.92
(1j)$_2$Ag	148	2170	25.93	0.54	15.18
		2130	26.07	0.69	15.33
(1k)$_2$Cu	175	2110	24.46	0.51	14.17
			24.71	0.58	13.85
(1k)$_2$Ag	163	2140	23.16	0.49	13.51
			23.44	0.56	15.31

[a] Calculated (above), found (below). − [b] IR (KBr): total absorption between 4000−600 cm^{-1}.

Radical-Anion Salts (DCNQI)$_2$M by Electrocrystallization. − General Procedure 4 (GP4): Three- (C3)[51] or two- (C2) -compartment[52] cells were used with a Pt cathode (either plates, 2 cm^2 or rods, diameter = 1 mm, *l* = 5 mm, ca. 0.17 cm^2) for different current densities. Anodes were rods from platinum or glassy carbon (Fa. Sigri). Electrolysis was run at constant current in degassed acetonitrile under argon (C3 = 60 mL, C2 = 80 mL) containing *x* μmol of DCNQI 1 and *y* μmol of supporting electrolyte [A = RbClO$_4$; B = CF$_3$CO$_2$Tl; C =Cu(CH$_3$CN)$_4$ClO$_4$; D = AgNO$_3$]. The radical salts which deposited in black shiny (thin) needles were harvested before all the DCNQI had been reduced, washed with MeCN and pentane and dried (see Table 4). Periodical switching between reduction and partial oxidation was performed with a home-made apparatus (B. Brunner) according to a circuit diagram given in the Supporting Information.

(1a)$_2$Cu: 1a (130 mg, 600 μmol), C (229 mg, 700 μmol), C2; 9 μA; Pt rod (53 μA cm^{-2}), switching 7:3/s, 5°C, 264 h. (1a)$_2$Cu (29.0 mg, 20%), m.p. 220°C (dec.). − IR (KBr): ṽ = 4000−600 cm^{-1}, total

absorption. − [C$_{10}$H$_8$N$_4$O$_2$]$_2$Cu (495.9): calcd. C 48.43, H 3.26, N 22.60; found C 48.44, H 3.22, N 23.05.

(1a)$_2$Rb: 1a (43.2 mg, 200 µmol), A (185 mg, 1.0 mmol), C3; 5 µA; Pt plate (2.5 µA cm^{-2}), −18 °C, 117 h. (**1a**)$_2$Rb (15.2 mg, 29%), m.p. 167 °C (dec.). − IR (KBr): ṽ = 2140 cm^{-1}, 2090 (C≡N). − [C$_{10}$H$_8$N$_4$O$_2$]$_2$Cu (517.9): calcd. C 46.38, H 3.12; N 21.64; found C 46.24, H 3.14, N 21.38.

(1b)$_2$Cu: 1b (120 mg, 600 µmol), C (229 mg, 700 µmol), C3; 9 µA; Pt rod (53 µA cm^{-2}), 22 °C, 97 h. (**1b**)$_2$Cu (32.0 mg, 23%), m.p. 158 °C (dec.). − IR (KBr): ṽ = 4000−600 cm^{-1}, total absorption. − [C$_{10}$H$_8$N$_4$O]$_2$Cu (463.9): calcd. C 51.77, H 3.48, N 24.16; found C 51.61, H 3.67, N 23.81.

(1c)$_2$Tl: 1c (36.8 mg, 200 µmol), B (64 mg, 200 µmol), C2; 30 µA, Pt plate (15 µA cm^{-2}); −18 °C, 72 h. (**1c**)$_2$Tl (27.1 mg, 48%), m.p. 161 °C (dec.). − IR (KBr): ṽ = 2120 cm^{-1}, 2080 (C≡N). − [C$_{10}$H$_8$N$_4$]$_2$Tl (572.7): calcd. C 41.93, H 2.82, N 19.57; found C 41.84, H 2.78, N 19.64.

(1d)$_2$Cu: 1d (44.1 mg, 200 µmol), C (98 mg, 300 µmol); C2; 10 µA, Pt rod (59 µA cm^{-2}); 20 °C, 72 h. (**1d**)$_2$Cu (17.1 mg, 34%), m.p. 180 °C (dec.). − IR (KBr): ṽ = 4000−600 cm^{-1}, total absorption. − [C$_9$H$_5$N$_4$ClO]$_2$Cu (504.8): calcd. C 42.82, H 2.00, N 22.20; found C 42.75, H 1.92, N 21.79.

(1e)$_2$Cu: 1e (53.0 mg, 200 µmol), C (98 mg, 300 µmol); C2; 10 µA, Pt rod (59 µA cm^{-2}); 20 °C, 72 h. (**1e**)$_2$Cu (23.1 mg, 39%), m.p. 196 °C (dec.). − IR (KBr): ṽ = 4000−600 cm^{-1}, total absorption. − [C$_9$H$_5$N$_4$BrO]$_2$Cu (563.7): calcd. C 36.41, H 1.70, N 18.88; found C 36.48, H 1.72, N 18.77.

(1f)$_2$Cu: 1f (94 mg, 300 µmol), C (195 mg, 600 µmol); C2; 9 µA, Pt rod (53 µA cm^{-2}), switching 7:3/s, 20 °C, 14 d. (**1f**)$_2$Cu (10.0 mg, 8%) − IR (KBr): ṽ = 4000−600 cm^{-1}, total absorption. − C$_{18}$H$_{10}$CuI$_2$N$_8$O$_2$ (687.7): calcd. C 31.44, H 1.47, N 16.29; found C 30.60, H 1.37, N 15.81.

(1h)$_2$Tl: 1h (74.4 mg, 300 µmol), B (95 mg, 300 µmol); C2; 20 µA, Pt plate (10 µA cm^{-1}), −18 °C, 44 h. (**1h**)$_2$Tl (15.1 mg, 22%), m.p. 106 °C (decomposition within 4 d). − IR (KBr): ṽ = 2130 cm^{-1}, 2090 (C≡N). − [C$_9$H$_5$N$_4$Br]$_2$Tl (702.5): calcd. C 31.05, H 1.30, N 15.60; found C 30.77, H 1.44, N 15.95.

(1i)$_2$Tl: 1i (59.2 mg, 200 µmol), B (95 mg, 300 µmol); C2; 25 µA, Pt plate (12.5 µA cm^{-2}), −18 °C, 44 h. (**1h**)$_2$Tl (15.1 mg, 22%), m.p. 111 °C (dec.).− IR (KBr): ṽ = 2090 cm^{-1} (C≡N). − [C$_9$H$_5$N$_4$I]$_2$Tl (976.5): calcd. C 27.14, H 1.27, N 14.07; found C 27.13, H 1.30, N 14.08.

(1j)$_2$Cu: 1j (95.0 mg, 300 µmol), C (98 mg, 300 µmol); C2; 9 µA, Pt rod (53 µA cm^{-2}), 20 °C, 72 h. (**1j**)$_2$Cu (30.0 mg, 29%), m.p. 209 °C (dec.).− IR (KBr): ṽ = 4000−600 cm^{-1}, total absorption. − [C$_8$H$_2$N$_4$ClI]$_2$Cu (696.5): calcd. C 27.59, H 0.58, N 16.09; found C 28.08, H 0.72, N 16.01.

(1k)$_2$Cu: 1k (108 mg, 300 µmol), C (147 mg, 450 µmol); C2; 9 µA, Pt rod (53 µA cm^{-2}), 20 °C, 144 h. (**1h**)$_2$Cu (59.0 mg, 50%), m.p. 228 °C (dec.). − IR (KBr): ṽ = 4000−600 cm^{-1}, total absorption. − [C$_8$H$_2$N$_4$BrI]$_2$Cu (785.4): calcd. C 24.47, H 0.51, N 14.27; found C 24.71, H 0.66, N 13.82.

(1k)$_2$Ag: 1k (36.1 mg, 100 µmol), D (34 mg, 200 µmol); C3; 10 µA, Pt plate (5 µA cm^{-2}), −25 °C, 153 h. (**1k**)$_2$Ag (17.1 mg, 21%), m.p. 164 °C (dec.). − IR (KBr): ṽ = 2180 cm^{-1}, 2140 (C≡N). − [C$_8$H$_2$N$_4$BrI]Ag (829.8): calcd. C 23.16, H 0.49, N 13.51; found C 23.77, H 0.62, N 13.58.

(1l)$_2$Cu: 1l (81.6 mg, 200 µmol), C (98 mg, 300 µmol),; C2; 9 µA, Pt rod (53 µA cm^{-2}), 20 °C, 135 h. (**1l**)$_2$Cu (39.0mg, 45%), m.p.

201 °C (dec.). − IR (KBr): ṽ = 4000−600 cm^{-1}, total absorption. − [C$_8$H$_2$N$_4$I$_2$]$_2$Cu (879.4): calcd. C 21.85, H 0.46, N 12.74; found C 22.01, H 0.32, N 12.51.

DCNQI Radical-Anion Copper Salts Grown from Two Different DCNQIs on a Copper Wire: Two different DCNQIs **1** (100 µmol each) and copper(II) bromide (150 µmol) were dissolved in acetonitrile (25 mL) saturated with argon. According to GP3 (vide supra) a copper wire was immersed and after 3−5 d the dark needles (1−20 mm) which had formed were harvested. All specimens showed total absorption in their IR spectra between 4000−600 cm^{-1}. For details see Table 5.

DCNQI Radical-Anion Copper Salts with different DCNQI Ligands by Electrocrystallization: Following GP4 (vide supra) a pair of DCNQIs was applied in various ratios. The harvested needles (5−20 mm long, diameter 5−15 µm) appeared similar to those grown from one DCNQI only and showed total absorption in their IR spectra between 4000−600 cm^{-1}. For details see Table 6.

Acknowledgments

[1] Part LXVI: M. Hemmerling, S. Hünig, M. Kemmer, K. Peters, *Eur. J. Org. Chem.* **1998**, 1989−1996.
[2] H. Meixner, Ph.D. Thesis, University of Würzburg, **1991**; K. Sinzger, Ph.D. Thesis, University of Würzburg, **1995**.
[1] F. Wudl, D. Wobschall, E. J. Hufnagel, *J. Am. Chem. Soc.* **1972**, *94*, 670.
[2] J. Ferraris, D. O. Cowan, V. Walatka, Jr., J. H. Perlstein, *J. Am. Chem. Soc.* **1973**, *95*, 948.
[3] L. B. Coleman, M. J. Cohen, D. J. Sandman, F. G. Yamagishi, A. F. Garito, A. J. Heeger, *Solid State Commun.* **1973**, *12*, 1125.
[4] Cf.: J. M. Williams, J. R. Ferraro, R. J. Thorn, K. D. Carlson, U. Geiser, H. H. Wang, A. M. Kini, M.-H. Whangbo, *Organic Conductors (Including Fullerenes). Synthesis, Structure, Properties and Theory*, Prentice Hall, Englewood Cliffs, NJ, **1992**, p. 115.
[5] A. Aumüller, P. Erk, S. Hünig, G. Klebe, J. U. von Schütz, H.-P. Werner, *Angew. Chem.* **1986**, *98*, 760−761; *Angew. Chem. Int. Ed. Engl.* **1986**, *25*, 740−741.
[6] Review: S. Hünig, *J. Mater. Chem.* **1995**, *5*, 1469−1479.
[7] Cf. also: N. Martin, J. L. Segura, C. Seoane, *J. Mater. Chem.* **1997**, *7*, 1661−1676.
[8] Part LXIII: S. Hünig, R. Bau, M. Kemmer, T. Metzenthin, K. Peters, K. Sinzger, J. Gulbis, *Eur. J. Org. Chem.* **1998**, 335−348.
[9] A. Aumüller, P. Erk, S. Hünig, H. Meixner, J. U. von Schütz, H.-P. Werner, *Liebigs Ann. Chem.* **1987**, 997−1006.
[10] P. Erk, S. Hünig, G. Klebe, M. Krebs, J. U. von Schütz, *Chem. Ber.* **1991**, 2005−2011.
[11] A. Aumüller, Ph.D. Thesis, University of Würzburg, **1985**.
[12] P. Erk, S. Hünig, H. Meixner, J. U. von Schütz, H.-P. Werner, *Liebigs Ann. Chem.* **1988**, 157−159.
[13] R. C. Wheland, J. L. Gillson, *J. Am. Chem. Soc.* **1976**, *98*, 3916−3925.
[14] A. Aumüller, P. Erk, H. Meixner, S. Hünig, J. U. von Schütz, H.-J. Gross, U. Langohr, H.-P. Werner, H. C. Wolf, C. Burschka, G. Klebe, K. Peters, H. G. von Schnering, *Synth. Met.* **1988**, *27*, B 181−188.
[15] R. Kato, H. Kobayashi, A. Kobayashi, T. Mori, H. Inokuchi, *Chem. Lett.* **1987**, 1579−1582.
[16] H. Kobayashi, R. Kato, A. Kobayashi, T. Mori, H. Inokuchi, *Solid State Commun.* **1988**, *65*, 1351−1354.
[17] L. R. Melby, *Can. J. Chem.* **1965**, *43*, 1448.
[18] P. Erk, Ph.D. Thesis, University of Würzburg, **1989**.
[19] A. Kobayashi, T. Mori, H. Inokuchi, R. Kato, *Synth. Met.* **1988**, *27*, B275−280.
[20] S. Hünig, H. Meixner, T. Metzenthin, U. Langohr, H. U. von Schütz, H. C. Wolf, E. Tillmanns, *Adv. Mater.* **1990**, *2*, 361−363.

[21] H. W. Helberg, personal communication, March **1991**.

[22] [22a] S. Hünig, *Pure Appl. Chem.* **1990**, *62*, 395−406. − [22b] S. Hünig, P. Erk, *Adv. Mater.* **1991**, *3*, 225−236.

[23] P. Erk, H. Meixner, T. Metzenthin, S. Hünig, U. Langohr, J.-U. von Schütz, H.-P. Werner, H. C. Wolf, R. Burkert, G. Schaumburg, H. W. Helberg, *Adv. Mater.* **1991**, *3*, 311−315.

[24] R. Kato, H. Kobayashi, A. Kobayashi, *J. Am. Chem. Soc.* **1989**, *111*, 5224−5232.

[25] A. Aumüller, P. Erk. S. Hünig, J. U. von Schütz, H.-P. Werner, H. C. Wolf, G. Klebe, *Mol. Cryst. Liq. Cryst. Inc. Nonlin. Opt.* **1988**, *156*, 215−221.

[26] T. Bauer, E. Tillmanns, S. Hünig, H. Meixner, T. Metzenthin, U. Langohr, H. Rieder, J. U. von Schütz, H. C. Wolf, *Acta Crystallogr.* **1991**, *A46*, C362.

[27] R. Kato, H. Kobayashi, A. Koboyashi, T. Mori, H. Inokuchi, *Synth. Met.* **1988**, *27*, B263−B268.

[28] Preliminary publication: H. J. Gross, U. Langohr, J. U. von Schütz, H.-P. Werner, H. C. Wolf, S. Tomic, D. Jérome, P. Erk, S. Hünig, H. Meixner, *J. Phys. (Paris)* **1989**, *50*, 2347−2355; P. Erk, S. Hünig, H. J. Gross, U. Langohr, H. Meixner, H.-P. Werner, J. U. von Schütz, H. C. Wolf, *Angew. Chem.* **1989**, *101*, 1297−1298; *Angew. Chem. Int. Ed. Engl.* **1989**, *28*, 1245−1246.

[29] A. Aumüller, S. Hünig, *Liebigs Ann. Chem.* **1986**, 165−176.

[30] A. Aumüller, P. Erk, S. Hünig, H. Meixner, J. U. von Schütz, H.-P. Werner, *Liebigs Ann. Chem.* **1987**, 997−1006.

[31] A. Kobayashi, R. Kato, H. Kobayashi, *Synth. Met.* **1991**, *42*, 1769−1774; A. Kobayashi, R. Kato, H. Kobayashi, *Chem. Lett.* **1989**, 1843−1646.

[32] See also ref.[28]

[33] K. Sinzger, S. Hünig, M. Jopp, D. Bauer, W. Bietsch, J. U. von Schütz, H. C. Wolf, R. K. Kremer, T. Metzenthin, R. Bau, S. I. Khan, A. Lindbaum, C. L. Lengauer, E. Tillmanns, *J. Am. Chem. Soc.* **1993**, *115*, 7696−7705.

[34] S. Hünig, K. Sinzger, M. Jopp, D. Bauer, W. Bietsch, J. U. von Schütz, *Angew. Chem.* **1992**, *104*, 896−899; *Angew. Chem. Int. Ed. Engl.* **1992**, *31*, 859−862.

[35] [35a] A. J. Epstein, E. M. Conwell, *Solid State Commun.* **1977**, *24*, 627−630. − [35b] J. S. Miller, A. J. Epstein, *Angew. Chem.* **1987**, *99*, 332−339; *Angew. Chem. Int. Ed. Engl.* **1987**, *26*, 287.

[36] S. Hünig, P. Erk, E. Günther, H. Meixner, T. Metzenthin, J. U. von Schütz, M. Bair, H.-J. Gross, U. Langohr, S. Söderholm, H.-P. Werner, H. C. Wolf, E. Tillmanns, *Synth. Met.* **1991**, *42*, 1781−1789.

[37] R. Moret, P. Erk, S. Hünig, J. U. von Schütz, *J. Phys. (Paris)* **1988**, *49*, 1925−1931.

[38] R. E. Peierls, *Quantum Theory of Solids*, Oxford University Press, Oxford, **1955**, p. 108.

[39] H.-P. Werner, J. U .von Schütz, H. C. Wolf, R. K. Kremer, M. Gehrke, A. Aumüller, P. Erk, S. Hünig, *Solid State Commun.* **1989**, *69*, 1127−1130.

[40] R. Bozio, C. Pecile, *Spectroscopy of Advanced Materials* (Eds.: R. J. H. Clark, R. E. Hester), John Wiley, Chichester, **1990**; M. Meneghetti, G. Lunardi, R. Bozio, C. Pecile, *Synth. Met.* **1991**, *42*, 1775−1780.

[41] Earlier measurements: [2,5-Me$_2$DCNQI]$_2$M; M = Li: J. U. von Schütz, M. Bair, H.-P. Werner, H. C. Wolf, A. Aumüller, P. Erk, S. Hünig, in *Organic and Inorganic Low Dimensional Crystalline Materials* (Eds.: P. Delhaes, M. Drillon), Plenum Press, Oxford, **1987**; R. Kato, H. Kobayashi, A. Kobayashi, T. Mori, H. Inokuchi, *Synth. Met.* **1988**, *27*, B263−B268; R. Kato, H. Kobayashi, A. Kobayashi, *Chem. Lett.* **1987**, 1579−1582; Na, K: M. Helmle, J. Reiner, U. Rempel, M. Mehring, J. U. von Schütz, P. Erk, S. Hünig, H. Meixner, *Synth. Met.* **1991**, *42*, 1763−1768; Rb: D. Schmeißer, P. Bätz, W. Göpel, W. Jaegermann, C. Pettenkofer, H. Wachtel, A. Jimenez-Gonzales, J. U. von Schütz, H. C. Wolf, J. Taborski, V. Wüstenhagen, E. Umbach, P. Erk, S. Hünig, H. Meixner, *Ber. Bunsenges. Phys. Chem.* **1991**, *95*, 1442−1443.

[42] S. Hünig, P. Erk, *Adv. Mater.* **1991**, *3*, 225−236.

[43] J. C. Carter, L. H. Benett, D. H. Kahan, "Metallic Shift in NMR", *Progress in Material Science*, vol. 20, part I, Pergamon Press, Oxford, **1977**.

[44] S. Tomic, D. Jérome, A. Aumüller, P. Erk, S. Hünig, J. U. von Schütz, *J. Phys. C: Solid State Phys.* **1982**, *21*, L203−207. S. Tomic, D. Jérome, A. Aumüller, P. Erk, S. Hünig, J. U. von Schütz, *Synth. Met.* **1988**, *27*, B281.

[45] D. Bauer, J. U. von Schütz, H. C. Wolf, S. Hünig, K. Sinzger, R. K. Kremer, *Adv. Mater.* **1993**, *5*, no. 11, 829−834.

[46] D. Gómez, J. U. von Schütz, H. C. Wolf, S. Hünig, *J. Phys. I* **1996**, *6*, 1655−1671.

[47] [47a] H. M. Rietveld, *Acta Crystallogr.* **1967**, *22*, 151−152. − [47b] H. M. Rietveld, *J. Appl. Crystallogr.* **1969**, *2*, 65−71.

[48] Th. Bauer, M.Sc. Thesis, University of Würzburg, **1990**.

[49] Powder Diffraction File, International Centre for Diffraction Data, Newtown, Newtown Square, PA, USA, **1996**.

[50] F. Lux, S. Trebert Haeberlin, W. Erhardt, *Fresenius Z. Anal. Chem.* **1986**, *323*, 833.

[51] D. Jérome, personal communication to P. Erk, **1989**.

[52] M. L. Kaplan, *J. Cryst. Growth* **1976**, *33*, 161−164; D. Schweitzer, personal communication to A. Aumüller, **1984**.